AD-A146 469 AN EXTENSION OF THE BORN INVERSION METHOD TO A DEPTH DEPENDENT REFERENCE..(U) COLORADO SCHOOL OF MINES GOLDEN CENTER FOR WAVE PHENOMENA N BLEISTEIN ET AL. 1/1

UNCLASSIFIED 01 AUG 84 CWP-007 N00014-84-K-0049 F/G 20/1 NL

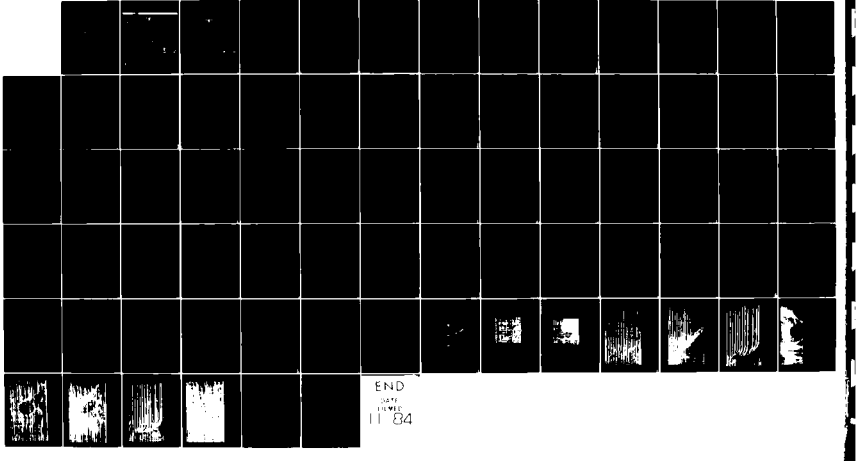

END
DATE FILMED
11 84

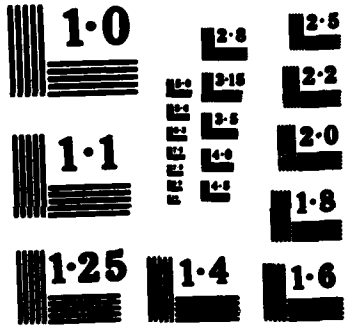
1·0
1·1
1·25
1·4
1·6
2·0
2·2
2·5

(12)

CSM

AD-A146 469

AN EXTENSION OF THE BORN INVERSION METHOD TO A DEPTH DEPENDENT REFERENCE PROFILE

Norman Bleistein* and Samuel H. Gray**

Supported by the Amoco Production Company
and by
The Selected Research Opportunities Program
of the
Office of Naval Research

Colorado School of Mines
Golden, Colorado 80401

Center for Wave Phenomena
Department of Mathematics

303/273-3557

CSM-007

AN EXTENSION OF THE BORN INVERSION METHOD TO A DEPTH DEPENDENT REFERENCE PROFILE

Norman Bleistein* and Samuel H. Gray**

Supported by the Amoco Production Company
and by
The Selected Research Opportunities Program
of the
Office of Naval Research

* Center for Wave Phenomena, Department of Mathematics, Colorado School of Mines, Golden, Colorado 80401

** Amoco Research Center, P. O. Box 591, Tulsa, Oklahoma 74102

CONTENTS

For a depth dependent reference speed, c(z), we can no longer invert the integral equation exactly. However, we can write down an asymptotic high frequency approximation for the kernel of the integral equation and an asymptotic solution for the perturbation. The computer implementation of this result is designed along the same lines as the code for the constant background case. In tests of processing time, we find that, at worst, the total processing time for this algorithm with depth dependent background soundspeed is about the same as for a comparably programmed k-f algorithm with constant background. By worst we mean that we choose the aspect ratio -- the number of traces divided by the number of points per trace -- to be optimal for the k-f algorithm. We present examples which demonstrate the method implemented as a migration technique and compare with the application of alternative migration algorithms. The examples we chose were ones in which the objective is to image the flanks of a salt dome.

ABSTRACT

The purpose of this paper is to describe an extension of the multidimensional Born inversion technique [Cohen and Bleistein, 1979a] for acoustic waves. In that earlier work, a perturbation in reference soundspeed was determined by assuming that the reference or background speed was constant. In this extension, we allow the reference speed to be a function of the depth variable, z, but still require that it be independent of the transverse variables. The output of this method is a high frequency bandlimited reflectivity function of the subsurface. The reflectivity function is an array of bandlimited singular functions scaled by the normal reflection strength. Each singular function is a Dirac delta function of a scalar argument which measures distance normal to a reflecting interface. Thus, the reflectivity function is an indicator map of subsurface reflectors which is equivalent to the map produced by migration. In addition to the assumption of small perturbation, the method requries the assumption that the reflection data reside in the high frequency regime, in a well-defined sense.

The method is based on the derivation of an integral equation for the perturbation in soundspeed from a known reference speed. When the reference speed is constant, the integral equation admits an analytic solution as a multifold integral of the reflection data. Further high frequency asymptotic analysis simplifies this integral considerably and leads to an extremely efficient numerical algorithm for computing the reflectivity function. In a paper by Bleistein, Cohen and Hagin [1984], the development of a computer code to implement this constant reference speed solution is described.

$w(\xi,\zeta)$	output of inversion operator applied to $U_S(\underline{k},0;\omega)$. Eq. (16).
$v(x,z)$	total soundspeed. Eq. (3).
$\underline{\xi} = (\xi,\eta,0)$	source/receiver location on upper surface.

GLOSSARY

$a(x,z)$ soundspeed perturbation. Eq. (3).

$\beta(\xi,\zeta)$ reflectivity function. Eq. (22).

$c(z)$ reference soundspeed. Eq. (3).

$f_{\pm}$ minimum(-) and maximum(+) frequencies of the data in Hz.

$\phi = \operatorname{sgn}\omega \int_0^z \mu_z(z',\underline{\mu};\omega)\,dz'$. Eq. (9).

$\underline{k} = (k_1,k_2)$ transverse Fourier transform variable.

$k = |\underline{k}| = \sqrt{k_1^2 + k_2^2}$

$\underline{\lambda} = (\lambda_1,\lambda_2)$ transverse Fourier transform variable.

$\lambda = |\underline{\lambda}|$

$\underline{\mu} = (\mu_1,\mu_2)$ transverse Fourier transform variable.

$\mu = |\underline{\mu}|$

$\mu_z = \sqrt{\omega^2/c^2 - \mu^2}$ vertical wave number defined locally in z by dispersion relation, Eq. (9).

ω frequency variable

p ray parameter. Eq. (25).

$\tau(\zeta,p)$ traveltime of inversion operator. Eq. (25).

$u(x,y,z;\omega)$ total field in frequency domain. Eq. (2).

$U(x,y,z;t)$ total field in time domain.

$u_I(x,y,z;\omega)$ incident field in frequency domain; response to point source with soundspeed $c(z)$. Eq. (4).

$U_I(x,y,z;t)$ u_I in the time domain.

$u_s(x,y,z;\omega)$ scattered field in the frequency domain; response to the perturbation, a. Eq. (5).

$U_s(x,y,z;t)$ u_s in the time domain.

$\tilde{u}_s(\underline{k},0;\omega)$ transverse Fourier transform of $u_s(\underline{\xi},0;\omega)$. Eq. (11).

1. INTRODUCTION

The purpose of this paper is to describe an extension of the Born inversion technique [Cohen and Bleistein, 1979a]. In that paper, a method was developed to determine the perturbation in soundspeed from a known reference speed. A closed form solution was derived when the reference speed was taken to be constant. In this extension, we allow the reference speed to be a function of the depth variable z, but we require that it be independent of the transverse variables (laterally homogeneous). The perturbation is allowed to be a function of all three spatial variables when a planar survey on the upper surface is available; it is allowed to be a function of one transverse variable and depth when only a line of surface data is available. We shall refer to this latter case of three dimensional propagation over an earth with two dimensional variations as the two and-one-half dimensional case; we shall refer to the former as the three dimensional case. In both cases, the surface observations we use are backscattered (CMP stacked) time logs.

Let us denote the soundspeed by $v(x,y,z)$. We introduce the reference speed, c, and a perturbation, a, in the form

$$\frac{1}{v^2} = \frac{1}{c^2}(1 + a) \tag{1}$$

The main features of the method are as follows:

(i) The method starts from the wave equation and a nonlinear integral equation for $a(x,y,z)$ is derived. The equation is nonlinear

because it contains the product of the perturbation and the unknown interior wave field.

(ii) Linearization, under the assumption that α is "small," leads to an integral equation for α in which the data are the ensemble of backscatter (coincident source-receiver) observations on the upper surface. The kernel of the integral equation is the square of a Green's function for the unperturbed problem with reference speed $c(z)$.

(iii) For constant c, the integral equation admits a closed form solution for α as a multi-fold integral of the observed data [Cohen and Bleistein, 1979]. Asymptotic analysis [Bleistein, Cohen and Hagin, 1984; referred to as BCH, below] reduces the number of integrations which must be performed by computer so that the processing times are competitive with, or better than, times for existing migration codes. (See Gray, [1984].) For depth-dependent c, the integral equation admits an approximate (asymptotic) solution, again as a multi-fold integral of the data. As with the case of constant c, asymptotic analysis greatly simplifies the computer implementation.

(iv) The computer implementation takes account of the fact that real seismic data is bandlimited in frequency. The method also employs constraints which account for causality and avoid aliasing in the transverse.

The output of this method is a high frequency bandlimited <u>reflectivity</u>

function of the subsurface. The reflectivity function is an array of bandlimited singular functions scaled by the normal incidence reflection strength. Each singular function is a Dirac delta function of a scalar argument which measures distance normal to a reflecting interface; see Fig. 1.

In characterizing this data as high frequency data we mean that the dimensionless parameter

$$\lambda = 4\pi fL/c$$

should be large. In this equation, f is the minimum frequency in Hz, c is the local soundspeed and L is a typical length scale. There is an extra factor of 2 in this equation due to the two-way travel time of interest in inverse problems; alternatively, c/2 may be viewed as the "migration velocity" for a problem where sources are set off at each reflector at time zero. The length scales of interest are the range from the upper surface to the reflecting surface, the principal radii of curvature of the reflector or the distance between reflectors. For the first two of these, a lower limit of 500m is reasonable. Let us consider a lower limit of frequency of 6 Hz and a soundspeed of 2000 m/sec. For this choice, $\lambda = 6\pi$ is much larger than necessary for high frequency asymptotic methods to be valid. In fact, a value of three (or π) will usually suffice. Thus, even an increase of velocity by a factor of 5 or a decrease in length scale by the same amount would leave λ large enough for asymptotic methods to apply. Unfortunately, small offset seismic data do not usually support resolution of layers whose

separation is such as to make λ less than three, whether or not we exploit high frequency techniques to invert the data.

The method has been checked on synthetic data in the two and-one-half dimensional case. The output of this inversion algorithm is a depth profile equivalent to one produced by a depth migration. The added feature of inversion is that the amplitude of the output provides an estimate of the velocity increments across the interfaces. The accuracy of this estimate can be no better than the accuracy of the input data as relative true amplitude data. However, in BCH, we show theoretically, using asymptotic analysis, that for true amplitude data the output provides a more accurate estimate of reflection strength at interfaces than its basis in perturbation theory would suggest. In the absence of true amplitudes, the output is fully equivalent to the output of a migration algorithm. In BCH, we discuss the relationship between inversion of both k-f migration [Stolt, 1978] and Kirchhoff migration [Schneider, 1978]. In order to distinguish the case in which parameter estimation is possible from the case in which it is not, we shall refer to the former as a seismic inversion and the latter as a structural inversion. Thus, from our point of view, migration is a structural inversion technique.

For a depth dependent reference speed, $c(z)$, we cannot invert the linearized integral equation exactly for a. We cannot even write down an exact analytical expression for the kernel of the integral equation, which is proportional to the square of a Green's function for the wave operator with soundspeed $c(z)$. However, we can write down an asymptotic (high frequency) approximation for this Green's function and an asymptotic

inversion of the integral equation for $a(x,y,z)$. Indeed, fundamental to this extension is early exploitation of asymptotics on the basis of high frequency in full anticipation of obtaining a solution only in the high frequency regime and only for the bandlimited reflectivity function. (This is much in the spirit of Clayton and Stolt [1981]). When the data is not relative true amplitude data, we lose only the estimate of reflection strength and this seismic inversion method remains a structural inversion method, now in the context of a depth dependent background soundspeed.

The computer implementation of this result is designed along the same general lines as the constant reference speed algorithm described in BCH. To obtain the output at a subsurface point, it is necessary to take the temporal Fourier transform of the range normalized data, multiply by a filter deduced by the theory, invert the transform, evaluate each trace at a traveltime deduced from the theory with an appropriate amplitude scale, and integrate over a set of traces. In the constant reference speed case, the traveltime and amplitude scales of the last integration are explicit functions of the integration point and the output point. In the $c(z)$ reference speed case, these latter functions are replaced by the geometrical optics traveltime and an amplitude on the ray connecting the subsurface output point and the source/receiver point in the context of the depth dependent reference profile. These functions are given implicitly in terms of a (ray) parameter which remains constant on a ray and is determined from the equation of the ray connecting the two points. We arbitrarily characterize the reference speed in this implementation as being piecewise linear and continuous, connecting prescribed values of soundspeed at prescribed depths in the subsurface. (For structural inversion, we could

just as easily prescribe the reference velocity to be piecewise constant. For seismic inversion, the piecewise constant background would required a more complicated amplitude in the inversion operator.) We compute the ray parameter and the necessary functions in advance and retain them in tables to be called as needed for the final integration of the algorithm.

Because these tables need only be computed once for each output depth (i.e., for each transverse offset separating output point and source/receiver location), the computing time for this part of the processing becomes a progressively smaller fraction of the total processing time as the aspect ratio -- the number of traces divided by the number of output points -- becomes larger. In tests of processing time we find that, at worst, the total processing time for this algorithm with depth dependent background velocity is about the same as for a comparably programmed k-f algorithm with constant background velocity. By worst, we mean that we choose both the number of traces and the number of points per trace to be a power of two and we choose the aspect ratio -- number of traces divided by number of points per trace -- to be optimal for the k-f algorithm.

Because of its implementation, described above, the method bears close relationship to one described by Carter and Frazer [1984]. The chief difference between them, other than algorithmic details, are: (1) Carter and Frazer's methods allows for transverse variations in c while ours does not; (2) our method allows for processing of true-amplitude data for reflection strength and hence velocity while Carter and Frazer's does not.

We present synthetic data examples which demonstrate the method

implemented as a structural inversion (migration) technique. For the simplest example of a single steeply tilted reflector, we compare this method with output of a k-f algorithm applied to a time-stretched version of the same data and to a Kirchhoff migration. We also present two examples in which the objective is to image the flanks of a salt dome intruding into an otherwise horizontally stratified medium. The advantages of the method of this type of application are evident from the output.

2. DERIVATION OF THE INTEGRAL EQUATION FOR ALPHA

We shall derive an integral equation for α. We assume that the time-reduced wavefield $u(\underline{x}, \omega)$ is a solution of the Helmholtz equation

$$\nabla^2 u + \frac{\omega^2}{v^2} u = -\delta(x - \xi)\, \delta(y - \eta)\, \delta(z) \quad . \tag{2}$$

In this equation, ∇^2 is the Laplace operator and δ is the Dirac delta function. This equation is to hold for all (x,y,z). It is further assumed that

$$\begin{aligned} \frac{1}{v^2} &= \frac{1}{c^2}(1 + \alpha) \quad , \quad z > 0,\ \alpha = \alpha(x,y,z),\ c = c(z)\ ; \\ \frac{1}{v^2} &= \frac{1}{c^2(0)} \quad , \quad z < 0\ . \end{aligned} \tag{3}$$

The function c(z) is the known continuous reference velocity and $\alpha(x,y,z)$ is the unknown perturbation to be determined from observations on the upper surface.

We introduce u_I, the solution of the unperturbed Helmholtz equation

$$\nabla^2 u_I + \frac{\omega^2}{c^2} u_I = -\delta(x - \xi)\,\delta(y - \eta)\,\delta(z) \quad . \tag{4}$$

The function u_I is often referred to as the "incident wave." Then we may write

$$u = u_I + u_S \quad ; \tag{5a}$$

$$\nabla^2 u_S + \frac{\omega^2}{c^2} u_S = -\frac{\omega^2}{c^2} \alpha [u_I + u_S] \quad . \tag{5b}$$

Let us suppose that α is small. Heuristically, since the "source term" $-(\omega^2/c^2)\alpha u$ in equation (5b) is $O(\alpha)$, we expect that the solution u_S is as well. Thus as a first approximation, we may neglect the product αu_S on the right side as being quadratic in α and hence of lower order than the product αu_I. Consequently, the linearized equation for u_S is

$$\nabla^2 u_S + \frac{\omega^2}{c^2} u_S = -\frac{\omega^2}{c^2} \alpha u_I \quad . \tag{6}$$

We shall now write down the Green's function representation for the solution u_S evaluated back at the source point; this is the backscatter response which is assumed to be the observed data. We remark that, from (2), the Green's function is just u_I itself, and the representation for u_S

is

$$u_S(\xi,\eta,0;\omega) = -\omega^2 \int_{-\infty}^{\infty} dx \int_{-\infty}^{\infty} dy \int_{0}^{\infty} dz \, \frac{\alpha(x,y,z)}{c^2(z)} \, u_I^2(x,y,z;\xi,\eta,0;\omega) \quad . \tag{7}$$

In this equation, we have used the fact that α is nonzero for $z < 0$ to integrate only over positive z values. Also, we have exhibited both sets of spatial arguments of u_I to emphasize its dependence upon both observation and integration coordinates. This is the integral equation for α; it is the first term in the Born series for u_S. We propose to solve this integral equation in the high frequency regime.

3. ANALYSIS OF THE INTEGRAL EQUATION FOR ALPHA

An exact analytical inversion of Eq. (7) for α is not generally available unless c is constant. Thus, we must content ourselves with an approximate solution which retains features of interest of the true velocity profile. As discussed in the introduction, we shall develop a <u>high frequency solution</u> for the reflectivity function under the assumption of a piecewise constant α.

We envision an inversion algorithm which, for output $\alpha(x,y,z)$, will be in the form of an integration over a set of traces whose transverse limits define some bounded interval about the transverse coordinate of the output or observation point - a Kirchhoff integral. Toward this end, we shall be content to replace u_I in (7) with a high frequency bandlimited approximation of that function for which the transverse offset is bounded. This approximation is the downward propagating WKB or geometrical optics approximate solution.

In Appendix A we derive such a solution as a Fourier integral. The result is

$$u_I(x,y,z;\xi,\eta,0;\omega) = -\frac{1}{4\pi^2 i}\int \frac{d\mu_1\, d\mu_2\ \exp\{i\underline{\mu}\cdot(\underline{x}-\underline{\xi}) + i\phi(z,\underline{\mu};\omega)\}}{\sqrt{\mu_3(z,\underline{\mu};\omega)\ \mu_3(0,\underline{\mu};\omega)}}\,. \qquad (8)$$

In this equation, we have introduced the following notation:

$$\underline{x} = (x,y),\ \underline{\mu} = (\mu_1,\mu_2),\ \phi = \operatorname{sgn}\omega \int_0^z \mu_3(z',\underline{\mu};\omega)\, dz' \quad ,$$

$$\mu_3(z,\underline{\mu},\omega) = \sqrt{\frac{\omega^2}{c^2(z)} - \mu^2}, \qquad \mu^2 = \mu_1^2 + \mu_2^2 \quad . \tag{9}$$

We do not concern ourselves here with the values of $\underline{\mu}$ for which the square root is zero or imaginary. The former case corresponds to rays at their turning point; the latter case corresponds to evanescent waves. We justify the first of these by the observation that, in our inversion formula, we shall artificially limit the range of transverse variables to preclude the turned rays, thus limiting the amount of dip which can be imaged to vertical, at most. We justify the latter by noting that, in fact, a is the Fourier inversion of its spatial transform over <u>real</u> wave vectors.

By using this representation for u_I in (9), we obtain the following approximate integral equation for a:

$$u_S(\xi,0;\omega) = \frac{\omega^2}{4(2\pi)^4} \int dx\, dy \int_0 dz\, \frac{\alpha(\underline{x},z)}{c^2(z)}$$

$$\cdot \int \frac{d\mu_1\, d\mu_2\, \exp\{i\underline{\mu}\cdot(\underline{x}-\underline{\xi}) + i\phi(z,\underline{\mu};\omega)\}}{\sqrt{\mu_3(z,\underline{\mu};\omega)\ \mu_3(0,\underline{\mu};\omega)}} \tag{10}$$

$$\cdot \int \frac{d\lambda_1\, d\lambda_2\, \exp\{i\underline{\lambda}\cdot(\underline{x}-\underline{\xi}) + i\phi(z,\underline{\lambda};\omega)\}}{\sqrt{\mu_3(z,\underline{\lambda};\omega)\ \mu_3(0,\underline{\lambda};\omega)}} \ .$$

In this equation, we have omitted limits of integration except for the lower limit in z. We take the point of view that the limits of integration in all integrals is the range of values that allows the square roots in the integrand to remain real.

Eq. (10) is the integral equation which we shall invert in the next section. We note that Eq. (10) is a "high frequency" approximation to Eq. (7), which is itself a "small α" approximation to the exact expression for $u_S(\xi,\eta,0;\omega)$. We also note that we shall invert in Eq. (10) only in an asymptotic sense. The validity of our cascade of approximations will be demonstrated by the numerical examples.

4. ASYMPTOTIC INVERSION OF THE INTEGRAL EQUATION

We shall now describe the (asymptotic) inversion of the integral equation (10). To begin, we introduce the spatial Fourier transform of u_S with respect to $\underline{\xi}$ defined by

$$U_S(\underline{k},0;\omega) = \int_{-\infty}^{\infty} d\xi\, d\eta\, u_S(\underline{\xi},0;\omega)\, \exp\{-2i\underline{k}\cdot\underline{\xi}\}\ , \quad \underline{k} = (k_1,k_2)\ . \tag{11}$$

By taking this Fourier transform in (10) we obtain the following equation:

$$\begin{aligned} U_S(\underline{k},0;\omega) = \frac{\omega^2}{16\pi^2} \int_{-\infty}^{\infty} dx \int_{-\infty}^{\infty} dy \int_0^{\infty} dz\, \frac{\alpha(\underline{x},z)}{c^2(z)} \\ \cdot \int \frac{d\mu_1\, d\mu_2\, \exp\{i\underline{\mu}\cdot\underline{x} + i\phi(z,\underline{\mu};\omega)\}}{\sqrt{\mu_3(z,\underline{\mu};\omega)\ \mu_3(0,\underline{\mu};\omega)}} \\ \cdot \int \frac{d\lambda_1\, d\lambda_2\, \exp\{i\underline{\lambda}\cdot\underline{x} + i\phi(z,\underline{\lambda};\omega)\}}{\sqrt{\mu_3(z,\underline{\lambda};\omega)\ \mu_3(0,\underline{\lambda};\omega)}}\, \delta(2\underline{k} + \underline{\lambda} + \underline{\mu})\ . \end{aligned} \tag{12}$$

In this result, we have used the fact that

$$\int_{-\infty}^{\infty} d\xi\, d\eta\, \exp\{-i\underline{k}\cdot\underline{\xi}\} = (2\pi)^2\, \delta(\underline{k})$$

The delta function in (12) now allows us to calculate the integral in $\underline{\lambda}$. (We could as easily use it to calculate the integral in $\underline{\mu}$.) The result is

$$W_g(\underline{k},0;\omega) = \frac{\omega^2}{16\pi^3} \int_{-\infty}^{\infty} dx \int_{-\infty}^{\infty} dy \int_0^{\infty} dz \int d\mu_1 \int d\mu_2\, \frac{a(x,y)}{c^2(z)} \exp\{-2i\underline{k}\cdot\underline{x}\}$$

$$\cdot \frac{\exp\{i[\phi(z,\underline{\mu};\omega) + \phi(z,2\underline{k}+\underline{\mu};\omega)]\}}{\sqrt{\mu_3(z,\underline{\mu};\omega)\, \mu_3(0,\underline{\mu};\omega)\, \mu_3(z,2\underline{k}+\underline{\mu};\omega)\, \mu_3(0,2\underline{k}+\underline{\mu};\omega)}} \,. \tag{13}$$

We shall calculate the $\underline{\mu}$ integral by the method of stationary phase [Bleistein, 1984]. The large parameter in this integral is again the high frequency, although that is not apparent in the given representation. It would become apparent if we were to scale $\underline{\mu}$ and $\underline{k}$ by $|\omega|$ and scale the depth by the depth to the first reflector. Then we would find the dimensionless depth to the first reflector, measured in wave lengths, emerging as a scale on the phase of the $\underline{\mu}$ integration and this would be the dimensionless large parameter. We do not do this, but proceed formally to use the method of stationary phase directly on the integral (13). This is carried out in Appendix B. The result is

$$\mathfrak{U}_S(\underline{k},0;\omega) = \frac{\omega}{16\pi i} \int_0^\infty \frac{dz\ \mathfrak{U}(\underline{k},z)\ \exp\{2i\phi(z,\underline{k};\omega)\}}{c^2(z)\ \mu_3(z,\underline{k};\omega)\ \mu_3(0,\underline{k};\omega)\ \sigma(z,\underline{k};\omega)} \quad . \tag{14}$$

In this equation,

$$\sigma(z,\underline{k};\omega) = \left[\int_0^z \frac{dz'}{\mu_3(z',\underline{k};\omega)} \int_0^z \frac{dz'}{c^2(z')\ \mu_3^3(z',\underline{k};\omega)} \right]^{1/2} . \tag{15}$$

When c(z) is replaced by a constant, the exponent in the integrand in (14) is simply $ik_3 z$, with

$$k_3^2 = \frac{\omega^2}{c^2} - k^2 \quad .$$

The integrand also simplifies significantly in this case. One then recognizes (14) as an equation for the Fourier transform with respect to z of $\mathfrak{U}$. The inversion of this transform to yield u is then straightforward. Awareness of this fact suggests an inversion which, at least asymptotically, has the same effect when c varies with depth. Thus, we define

$$w(\underline{\xi},\zeta) = \frac{16i}{\pi^2} \int \frac{d^2k\, d\omega\, \hat{u}_S(\underline{k},0;\omega)\, \exp\{-2i\phi(\zeta,\underline{k};\omega) + 2i\underline{k}\cdot\underline{\xi}\}}{\mu_s(\zeta,\underline{k};\omega)\, \operatorname{sgn}\omega} \quad . \tag{16}$$

We look upon w as the result of applying an integral operator to the (Fourier transformed) data in (14). By applying the same operator to the right side of (14), we find that

$$w(\underline{\xi},\zeta) = \frac{1}{\pi^3} \int_{-\infty}^{\infty} dx \int_{-\infty}^{\infty} dy \int_0^{\infty} dz \int dk_1 \int dk_2 \int \frac{\omega\, d\omega}{c^2(z)\, \mu_s(\zeta,\underline{k};\omega)}$$

$$\cdot \frac{a(\underline{x},z)\, \exp\{2i[\phi(z,\underline{k};\omega) - \phi(\zeta,\underline{k};\omega)] + 2i\underline{k}\cdot(\underline{\xi} - \underline{x})\}}{\mu_s(z,\underline{k};\omega)\, \mu_s(0,\underline{k};\omega)\, \sigma(z,\underline{k};\omega)} \tag{17}$$

For the case of constant c, the integrations on the right side can be carried out explicitly to yield the result

$$w(\underline{\xi},\zeta) = c\, a(\underline{\xi},\zeta)/\zeta; \qquad a(\underline{\xi},\zeta) = \zeta\, w(\underline{\xi},\zeta)/c \quad . \tag{18}$$

Thus at least for constant c, we see that the multifold integration on the data represented by w is in fact a multiple of a; that is, (16) and (18) provide a solution for a.

Our objective now is to carry out the integrations in (17) for the case of variable c. Again, we do so by using the method of stationary phase.

this time in the four variables $\underline{k}$ and $\underline{x}$. The remaining integrals in ω and z then become straightforward. This analysis is carried out in Appendix C. The result is

$$w(\underline{\xi},\zeta) = \frac{c(\zeta)\, c(0)\, a(\underline{\xi},\zeta)}{\int_0^\zeta c(z)\, dz} \quad , \tag{19}$$

which provides the solution for a:

$$a(\underline{\xi},\zeta) = \frac{w(\underline{\xi},\zeta)}{c(\zeta)\, c(0)} \int_0^\zeta c(z)\, dz \quad . \tag{20}$$

In order to write the solution for a in terms of the data observed at the upper surface, we use this result and the definition of w in (16) along with the definition of $\mathcal{U}$ in (11) and the definition of the time transform which placed us in frequency domain to begin with. The result is

$$a(\underline{\xi},\zeta) = \frac{16i \int_0^\zeta c(z)\, dz}{\pi^3\, c(\zeta)\, c(0)} \int dk_1 \int dk_2 \int d\omega \int_{-\infty}^{\infty} dx \int_{-\infty}^{\infty} dy \int_0^\infty dt$$

$$\cdot \frac{U_g(\underline{x},0,t)\, \exp\{2i[\underline{k}\cdot(\underline{\xi}-\underline{x}) - \operatorname{sgn}\omega \int_0^\zeta \mu_s(z,\underline{k};\omega)\, dz] + i\omega t\}}{\operatorname{sgn}\omega\, \mu_s(\zeta,\underline{k};\omega)} \tag{21}$$

In this equation, we have used the notation U_S to denote the upward scattered field in the time domain.

As mentioned in the introduction, we do not process the data to yield α itself, but to produce the reflectivity function or normal derivative of α, at each of the interfaces between the layers of constant α. The theory developed in Cohen and Bleistein [1979b] shows that we can processs for $\partial\alpha/\partial n$ by multiplying the integrand by $-2i\omega/c(\zeta)$, we can obtain β if, instead,we multiply by $-i\omega/2c(\zeta)$ before inverting. This is also discussed in BCH and in Bleistein [1984]. Thus, we introduce the reflectivity function $\beta(\xi,\zeta)$, obtained by multiplying the integrand in (21) by this factor. That is,

$$\beta(\xi,\zeta) = \frac{8\int_0^\zeta c(z)\,dz}{\pi^3 c^2(\zeta)\,c(0)} \int dk_1 \int dk_2 \int \omega\,d\omega \int_{-\infty}^{\infty} dx \int_{-\infty}^{\infty} dy \int_0^{\infty} dt \tag{22}$$

$$\cdot \frac{U_S(\underline{x},0,t)\,\exp\{2i[\underline{k}\cdot(\underline{\xi}-\underline{x}) - \operatorname{sgn}\omega \int_0^\zeta \mu_z(z,\underline{k};\omega)\,dz] + i\omega t\}}{\operatorname{sgn}\omega\,\mu_z(\zeta,\underline{k};\omega)}$$

In practice, an areal array of data, as is required for this formula, is not usually available; only a line of data at the upper surface is available, say in the direction of the x axis of our formulation. In order to treat this type of data, it is assumed that there is no variation in velocity in the orthogonal horizontal direction, namely the y direction. In that case, the data itself must be y-independent. This allows us to carry out the integrations in y and k_2. The former of these yields $\pi\,\delta(k_2)$ and the latter integration then yields a value of π while also evaluating the

integrand at $k_z = 0$. Consequently, we may replace k_z by k in the integrand and write down the following result for the reflectivity function in the case of y independence:

$$\beta(\xi,\zeta) = \frac{8\int_0^\zeta c(z)\,dz}{\pi\, c^2(\zeta)\, d(0)} \int dk \int \omega\, d\omega \int_{-\infty}^{\infty} dx \int_0^\infty dt \tag{23}$$

$$\cdot \frac{U_S(\underline{x},0,t)\, \exp\{2i[\, k(\xi - x) - \operatorname{sgn}\omega \int_0^\zeta \mu_z(z,k;\omega)\, dz] + i\omega t\}}{\operatorname{sgn}\omega\, \mu_z(z,k;\omega)} \cdot$$

Although β is assumed only to have two dimensional variability in this result, the wave field has three dimensional spreading properties. Thus, this is the formula for the <u>two and one-half dimensional case</u>. We remark that a fully two dimensional formalism (governed by a two dimensional wave equation) would not properly account for the "geometrical spreading" of a three dimensional environment as this two and one-half dimensional result does.

For the case of constant c, we can compare this formula to the result in Cohen and Bleistein [1979a]. This comparison is sufficiently complicated to carry out that we do so in Appendix D. To leading order asymptotically, they do, indeed, agree.

Also for constant c, (23) has the form of a k-f migration integral. In fact, when compared to Stolt [1978], equation (50), we find that we must

(i) interpret Stolt's φ as $tU_g(x,0,t)$ and (ii) integrate by parts with respect to ω as is done in Appendix D of this paper. Then the integrals are the same to leading order asymptotically for large ω up to a multiplicative constant. Since the Stolt k-f formula is migrating the field and we are producing β, this difference of a multiplier causes no difficulty. However, except for such constant multipliers, it is necessary that the integral processing agree, at least to leading order in ω, because both methods produce an image of the interfaces between layers. Only the interpretation of the intensity of the imaging function differs in the two methods.

5. ASYMPTOTIC REDUCTION TO A COMPUTER IMPLEMENTABLE FORMULA

The formula (23) is not easily implemented on the computer. Furthermore, in that formula, we have not fully exploited the possible simplifications available under the assumption of "high frequency." To achieve this end, there is still one integration which can be carried out asymptotically, namely, the integration in k, the transverse wave number. This calculation is carried out in Appendix E. The result of that calculation is

$$\beta(\xi,\zeta) = -\frac{32\int_0^\zeta c(z)\,dz}{\sqrt{\pi}\,c(0)\,c^2(\zeta)}\int\frac{dx}{\sqrt{n^2(\zeta)-p^2}\,S(\zeta,p)}$$

$$\cdot\int\sqrt{|\omega|}\,d\omega\,\exp\{-2i\omega\tau(p,\zeta)+i(\operatorname{sgn}\omega)\pi/4\} \qquad (24)$$

$$\cdot\int U_g(x,0,t)\exp\{i\omega t\}dt\ ,$$

$$|x-\xi| = p\int_0^\zeta\frac{dz}{\sqrt{n^2(z)-p^2}}\ ;\quad \tau(\zeta,p) = \frac{1}{c(0)}\int_0^\zeta\frac{n^2(z)\,dz}{\sqrt{n^2(z)-p^2}}\ ;$$

$$S(\zeta,p) = \left[\int_0^\zeta\frac{n^2(z)\,dz}{(n^2(z)-p^2)^{3/2}}\right]^{1/2}\ ,\quad n^2(z) = \frac{c^2(0)}{c^2(z)}\ . \qquad (25)$$

In these equations, the integrand is stated parametrically with parameter p. This is a dimensionless ray parameter which denotes the sine of the emergence angle with respect to the vertical of a reflected ray. (This

usage is a departure from the usage in the τ-p method where this parameter is divided by $c(0)$ but is also denoted by p.) For each choice of $|x - \xi|$ and ζ, we must determine the value of p from the first equation in (25). Given p, the values of $\tau(\zeta,p)$ and $S(\zeta,p)$ are then determined, as well as the explicit square root appearing in the integrand. The choice of τ determines a "time" at which the processed time logs (CDP stacked traces) are to be evaluated. "Processed" means Fourier transformed in time, multiplied by a function of ω and inverse Fourier transformed. The range of integration in space is restricted to those values of x for which the square roots of the integrand remain real and nonzero and the travel time τ remaining less than the maximum time on the set of traces.

Equations (24) and (25) are to be implemented on the computer. In anticipation of this, we have written our result in terms of n(z), the index of refraction, which is a number varying typically between .25 and 4, rather than in terms of the inverse velocity or slowness, which is three orders of magnitude smaller, with similar estimates true for the corresponding parameter p. The computer implementation proceeds as follows:

(i) Calculate the Fourier time transform of each trace.

(ii) Multiply by a function of the frequency variable, perform filtering as required and take the inverse Fourier transform. This inverse transform is now given on a uniform grid in time.

(iii) For fixed output depth ζ, develop a table of values of p as a function of $|x - \xi|$ (transverse offset between output point (ξ,ζ)

and receiver location (x,0)) for the prescribed reference velocity c(z). We use a table here because the same choices of these variables arise repeatedly in carrying out the spatial integration for different output points at the given depths.

(iv) With the p values determined, develop tables of the other functions of p, namely τ and S in Eq. (25), as well.

(v) Now for fixed (ξ,ζ), calculate the spatial integral as a discrete sum over the locations x of the traces, subject to the limits of summation noted above. Typically, the value of τ at a given choice of x, ξ and ζ will not be available in the table of processed data determined in (ii). Therefore, use an interpolation scheme to estimate the value of the processed data at τ in terms of the processed data at the grid points of the time variable.

The integration in ω is to be carried out over the available bandwidth of the data. The Fourier transform should not simply be truncated at the endpoints of the bandwidth, but a smoothing filter should be applied to avoid ringing of the output due to a discontinuous filter.

The spatial integration must also be further constrained by sampling rate considerations associated with the discreteness of data in the spatial domain. If this is not done, spatial aliasing will occur and will be apparent in the output. The requirement which we impose is that the transverse component of the wave vector in the phase of the x integral must

be bounded by the tranverse spatial Nyquist frequency associated with the sampling rate or spacing of the traces, as discussed next.

Let us denote the trace separation in the transverse by Δx. The transverse wave vector can be determined from the phase $2\omega\tau$ by calculating the partial derivative of that function with respect to x. This derivative is equal to the quotient of derivatives of $2\omega\tau$ and $|x - \xi|$ — with τ and $|x - \xi|$ defined in (25) — with respect to p at fixed ζ. That is,

$$2\omega \frac{\partial \tau}{\partial p} = \frac{\left[\frac{\partial \tau}{\partial p}\right]}{\left[\frac{\partial x}{\partial p}\right]} = 2\omega \frac{p}{c(0)} \tag{26}$$

We introduce the frequency in Hz, $f = \omega/2\pi$, and require that the transverse wave number satisfy our Nyquist bound even for the maximum frequency, say f_+. Then

$$\frac{2 \cdot 2\pi f_+ p}{c(0)} \leq \frac{2\pi}{2\Delta x} , \tag{27}$$

which leads to the condition

$$p \leq \frac{c(0)}{4 f_+ \Delta x} \quad . \tag{28}$$

This is the additional constraint on p which, in turn, imposes an additional constraint on the limits of integration (summation) in x.

The next question which arises is how to estimate the "jump" in α at an interface in terms of the reflectivity, β. This is discussed in Cohen and Bleistein [1979b] and Bleistein [1984] for the case of a "box" filter. Let us define $\Delta\alpha$ as the increment in α at such an interface and P as the peak value of β at an interface location on an output trace. The theory then predicts that

$$\Delta\alpha = P \cdot \frac{c(z)}{4(f_+ - f_-)} \quad . \tag{29}$$

In this equation, f_- is the minimum frequency.

For a more general filter, we must replace the difference of frequencies by the area under the filter functions, that is, if A denotes the area under the filter, then

$$\Delta\alpha = P \frac{c(z)}{4A} \quad . \tag{30}$$

Finally, there is some post-processing possible to compensate partially for the linearity of the underlying theory. This work was reported in Hagin and Cohen [1984]. We quote here the results of one important post-process and refer the reader to that paper for further detail.

In order to obtain an estimate of the velocity increment across an interface, one uses the linearized estimate deduced from (1),

$$\Delta c_{est} = -1/2\ c(z)\ \Delta\alpha \quad . \tag{31}$$

Here, Δc_{est} denotes the estimate obtained numerically. Hagin and Cohen then suggest as an improved estimate of the velocity increment

$$\Delta c = \frac{2c(z)\ \Delta c_{est}}{2c(z) - \Delta c_{est}} \quad . \tag{32}$$

We remark that all such post-processing refinements are only worthwhile if the original data is such that there is reason to believe that at least relative true amplitude was preserved. When this is not the case, such post-processing is unnecessary. Implementation of (24) and (25) still may be employed to yield a structural inversion or migration of the time logs.

6. ESTIMATE OF CPU TIME

We shall now discuss CPU time for the implementation of the five steps listed in the previous section. Let us define the following:

N_ξ The number of points in the transverse at which the output is to be calculated.

N_ζ The number of points in depth at which the output is to be calculated.

N_τ The number of time points on each input trace.

N_x The number of traces.

It should be noted here that, in practice, N_ζ is smaller than N_τ. The reason for this is that the sampling rate determines a Nyquist frequency which is usually larger than the maximum frequency of usable data. Thus, there is a limit to the resolution of the output based upon this maximum usable frequency and not on the sampling rate.

In our research, we have concluded that the density of the output need be no greater than to produce four points on the main lobe of the bandlimited delta functions which are being depicted. In Appendix F, this analysis is discussed. When those results are implemented with numbers typical of geophysical exploration data, we conclude that a typical value for the ratio N_ζ/N_τ is .56.

Implementation of each step of the previous section is estimated as follows:

Step (i) $O(N_x N_\tau \log_2 N_\tau)$ to compute the Fourier transforms.

Step (ii) $O(N_x N_\tau)$ to multiply all of the transforms by a function of frequency and then as in Step (i) to invert the Fourier transform.

Step (iii) $O(N_x N_\zeta)$ to develop the table of p values.

Step (iv) As in Step (iii).

Step (v) $O(N_\xi N_\zeta N_x')$ to calculate the final integral for the output.

In Step (v), we use N' to connote that, in fact, the aperture over which the integral is to be calculated is a fraction of the total number of traces - on average, perhaps one-half.

Steps (iii) and (iv) are computations which need not be performed in the case of constant c. We note that the "O" estimate for each of these steps can be significantly smaller than or comparable to the estimate for Step (v). This is so because N_x might be as large as N_ξ and N_x' may be a small fraction of N_ξ or, at most, equal to N_ξ.

7. EXAMPLES

We use three numerical examples both to illustrate the preceding theory and to demonstrate the differences between it and other migration methods. The first example is relatively simple; it will be used to provide a comparison of imaging methods. The second and third are more complicated and realistic.

Fig. 2(a) shows a synthetic time section from a dipping planar structure in a region where the velocity varies linearly with depth; the dip angle is 60 degrees and the velocity function is

$$c(z) = (5000 + 4z) \text{ ft/sec.} \tag{33}$$

The trace spacing is 50 ft. With c(z) taken as the reference velocity, the reconstruction as described in Section 5 is shown in Fig. 2(b). The time section has been correctly migrated; the apparent loss of high frequency content in the migration is due to imposing the constraint (28). For comparison, we show in Fig. 2(c) the results of a Kirchhoff migration of the same time section. Straight ray paths were assumed for this migration, and the traveltimes for diffraction curves were computed by using the rms velocity (converted from a function of time to a function of depth), as discussed by Schneider (1978). From this extreme example, which features a steeply dipping event and large background velocity variations, one can easily see the advantages of computing traveltimes along the curved ray paths defined implicitly in Eq. (25). The Kirchhoff output is incorrectly placed and the planar reflector is depicted as a curved surface. Additionally, a k-f migration was performed on this data after "stretching"

the time axis [Stolt, 1979]. This migration was totally unsuccessful in imaging the reflector. This is because, after the time axis was stretched, the reflection event on the resulting time section had an apparent dip greater than 45 degrees, making the migration equation

$$\sin(\text{migrated dip}) = \tan(\text{apparent dip}) \tag{34}$$

meaningless.

The second example (Fig. 3) shows a salt dome in a medium whose layering is otherwise nearly horizontal. Because the objective is to image the flanks of the salt dome and not its interior, migration with a reference velocity which varies with depth only is appropriate. Fig. 3(a) shows the model and Fig. 3(b) shows a finite-difference time section from the model. Part of the salt dome is overhung: its dip exceeds 90 degrees. The model velocity varies from 6000 ft/sec at the top of the model to 16000 ft/sec at the bottom; it is piecewise constant. The trace spacing is 100 ft. The reconstruction in Fig. 3(c) shows the correct imaging of dips up to, but not beyond, vertical. For a comparison with a reverse-time finite difference migration [Whitmore 1978], see Fig. 3(d) from Whitmore [1983]. The finite difference migration correctly images dips exceeding vertical, but its implementation is considerably more time-consuming than the approach studied here.

The third example also consists of a salt dome in a medium whose layering is otherwise nearly horizontal. The model is shown in Fig. 4(a), along with selected ray paths from reflecting interfaces to the upper surface. The model velocity varies from 5250 ft/sec at the top of the model to 14100 ft/sec at the bottom, and the trace spacing is 25 ft. We note that the ray paths are piecewise straight line segments, indicating that the model consists of piecewise constant-velocity layers, contrary to our specification of a continuous, piecewise linear, depth dependent velocity layering. Nevertheless, the migration (Fig. 4(b)) was successful. The most notable errors are:

(1) The inaccurate mapping of the interface directly below the salt dome. This occurred because the acoustic velocity of the salt is higher than that of the sediments, leading to reduced traveltimes for reflection events whose rays have travelled large distances through the salt. The one-dimensional reference velocity failed to account for this fact.

(2) The appearance of diffraction smiles on the migrated section. These are due to the artificial truncation of reflected energy on the time section; that is, the time section does not contain diffraction effects. This is, therefore, a limitation of the synthetic time data and not of the migration. In fact, any migration method will correctly interpret those truncated events as nearly circular reflector continuations. Finally, Fig. 4(d) shows the effects of modifying the anti-spatial-aliasing constraint (28). With the 4 in the denominator replaced by 8, spatial aliasing is further limited along with the ability to image the most steeply-dipping events (which appear on Fig. 4(a) as those most likely to be aliased).

Computer run times for these and other experiments indicate that the speed of this algorithm is about the same as that of a comparably coded (FORTRAN) k-f migration routine.

8. CONCLUSIONS

We have extended the multidimensional Born inversion formalism and algorithm to the case where the known reference velocity, from which perturbations are to be computed, are a function of depth. The analytical result has made use of a linearization (small perturbations from the reference velocity) and a high frequency assumption (that seismic data are frequency bandlimited, with even the lowest available frequencies considered to be "high" for the problem at hand). The reduction to an implementable algorithm has made further use of the high frequency assumption, resulting in an efficient structural inversion method.

ACKNOWLEDGEMENTS

We wish to thank Dan Whitmore for providing the finite-difference synthetic data, and Amoco Production Company for permission to publish these results.

This research project was initiated while the first author was a visitor at the Amoco Research Center in Tulsa during the months of February and March, 1983. This author wishes to express his deep appreciatiation to Amoco for providing a friendly and stimulating environment in which to work. There is no question in my mind that the quality of that environment contributed significantly to the success of this project.

REFERENCES

Bleistein, N., 1984, Mathematical Methods for Wave Phenomena: Academic Press, New York.

Bleistein, N., and Handelsman, R. A., 1975, Asymptotic Expansions of Integrals: Holt, Rinehart and Winston, New York; to be republished by Dover, New York, 1985.

Carter, J. A., and Frazer, L. N., 1984, Accommodating lateral velocity changes in Kirchhoff migration by means of Fermat's principle: Geophysics, 44, p. 46-53.

Clayton, R. W., and Stolt, R. H., 1981, A Born WKBJ inversion method for acoustic reflection data: Geophysics, 46, 11, 1559-1568.

Coddington E. A., and Levinson, N., 1955, The Theory of Ordinary Differential Equations: McGraw-Hill, New York.

Cohen, J. K., and Bleistein, N., 1979a, Velocity inversion procedure for acoustic waves: Geophysics, 44, 6, 1077-1085.

_____, 1979b, The singular function of a surface and physical optics inverse scattering: Wave Motion, 1, 153-161

Hagin, F. G., and Cohen, J. K., 1984, Refinements to the linear velocity inversion theory: Geophysics, to appear.

Schneider, W. A., 1978, Integral formulation for migration in two and three dimensions: Geophysics, 43, p. 49-76.

Stolt, R. H., 1978, Migration by Fourier transforms: Geophysics, 43, 1, 23-48.

Stolt, R. H., 1979, One more time: Stanford Exploration Project, 20, p. 197-200.

Whitmore, N. D., 1978, Depth migration by finite difference techniques: Amoco Production Company report.

Whitmore, N. D., 1983, Iterative depth migration by backward time propagation: Presented at 54th Annual SEG, Las Vegas.

APPENDIX A: ASYMPTOTIC DOWNGOING SOLUTION

The purpose of this appendix is to derive the asymptotic downgoing solution, (8), to equation (5). We begin by introducing the spatial Fourier transform of the solution, defined by

$$\tilde{u}(\underline{\mu},z;\omega) = \int_{\infty}^{\infty} u(\underline{x},z,\omega)\, \exp\{-i\underline{\mu}\cdot\underline{x}\}\, dx\, dy, \quad \underline{\mu} = (\mu_1,\mu_2) \tag{A-1}$$

By applying this Fourier transform to equation (5), we obtain the following ordinary differential equation for the function $\tilde{u}$:

$$\frac{d^2\tilde{u}}{dz^2} + \mu_3^2\, \tilde{u} = -\delta(z)\, \exp\{-i\underline{\mu}\cdot\underline{\xi}\} \quad ,$$
$$\mu_3(z,\underline{\mu};\omega) = \sqrt{\frac{\omega^2}{c^2(z)} - \mu^2}, \qquad \mu^2 = \mu_1^2 + \mu_2^2 < \frac{\omega^2}{c^2(z)} \quad . \tag{A-2}$$

We have only defined μ_3 for the ranges of its variables which make it real, and we shall only concern outselves with the asymptotic solution in that range as well.

Asymptotic theory for ordinary differential equations — see for example Coddington and Levinson [1955] -- indicates that two linearly independent solutions to the homogeneous form of (A2) are given asymptotically by

$$\tilde{u}_{\pm} \sim \frac{a_{\pm} \exp\{\pm i\phi(z;\omega) - i\,\underline{\mu}\cdot\underline{\xi}\}}{\sqrt{\mu_3(z,\underline{\mu};\omega)}}, \quad \phi = \operatorname{sgn}\omega \int_0^z \mu_3(z',\underline{\mu};\omega)\, dz' \tag{A-3}$$

In this equation, $a_{\pm}$ are constants. The solution $\tilde{u}_{+}$ is <u>outgoing</u> for $z \to \infty$ and the solution $\tilde{u}_{-}$ is <u>outgoing</u> for $z \to -\infty$. Since (5) is homogeneous for z nonzero, we conclude that

$$\tilde{u} = \tilde{u}_{\pm}, \quad \pm z > 0 \quad , \tag{A-4}$$

with only the constants $a_{\pm}$ to be determined.

In order to determine these constants, we must impose two conditions at $z = 0$, those conditions characterizing the distributional nature of the source. The conditions are that the function itself must be continuous and the first derivative of the function must have a "jump" equal to the integral of the right side on an interval containing the origin in z. These two equations are

$$\begin{aligned} a_{+} - a_{-} &= 0 \quad , \\ a_{+} + a_{-} &= -\frac{\exp\{-i\underline{\mu}\cdot\underline{\xi}\}}{i\sqrt{\mu_3(0,\underline{\mu};\omega)}} \quad , \end{aligned} \tag{A-5}$$

after a division of common factors. The sum of these equations yields a_{+}

which is the only constant of interest in our further discussion. Fourier inversion then yields equation (8).

APPENDIX B: ASYMPTOTIC EXPANSION OF (13)

The purpose of this appendix is to derive the result (14), which is the asymptotic expansion of the $\underline{\mu}$-integral in (13). We shall begin be reminding the reader of the basic multi-dimensional stationary phase formula. For a derivation, see Bleistein [1984], for example.

Let us suppose that $I(\lambda)$ is a multi-fold integral of the form

$$I(\lambda) = \int_D f(\underline{k}) \exp\{i\lambda\Phi(\underline{k})\}\, dk_1 \cdots dk_n \quad . \tag{B-1}$$

In this equation, D denotes some domain in $\underline{k}$ - space. The integral (13) is of this form in the variables $\underline{k}$ with $n = 2$. In a subsequent appendix, we shall have need of this result with $n = 4$. Our intention is to state the formula for the leading term of the asymptotic expansion of this integral for "large" values of the parameter, λ. As explained in the text, we have not recast the integral in a form in which λ is explicit. Therefore, we shall apply the formula below with $\lambda = 1$.

Let us suppose that, in D, $\underline{k}_o$ is the only <u>simple stationary point</u>, that is,

$$\nabla\Phi(\underline{k}_o) = \underline{0} \quad , \tag{B-2}$$

but the matrix with elements

$$\Phi_{ij} = \frac{\partial^2 \Phi(k_o)}{\partial k_i \partial k_j} \quad , \; i,j = 1, \cdots, n \; , \tag{B-3}$$

is nonsingular. Then, the leading term of the asymptotic expansion of the integral (B-1) is

$$I(\lambda) \sim \left[\frac{2\pi}{\lambda}\right]^{n/2} \frac{f(\underline{k}_o)}{\sqrt{|\det \Phi_{ij}|}} \exp\{i\lambda\Phi(\underline{k}_o) + i\pi(\operatorname{sgn} \Phi_{ij})/4\} \quad . \tag{B-4}$$

In this equation, $\operatorname{sgn} \Phi_{ij}$ is the <u>signature</u> of the matrix Φ_{ij}. The signature is the number of positive eigenvalues minus the number of negative eigenvalues of the matrix. If the domain D has more stationary points, one simply adds up the contributions from each of them.

Let us now consider the integral (13) and set

$$\Phi(\underline{\mu}) = \operatorname{sgn} \omega[\phi(z,\underline{\mu};\omega) + \phi(z,2\underline{k} + \underline{\mu};\omega)] \quad , \tag{B-5}$$

with ϕ defined by (9). Differentiation with respect to $\underline{\mu}$ yields the following results:

$$\frac{\partial \Phi}{\partial \mu_i} = -\operatorname{sgn}\omega \int_0^z \left[\frac{\mu_i}{\mu_s(z',\underline{\mu};\omega)} + \frac{2k_i + \mu_i}{\mu_s(z',2\underline{k} + \underline{\mu};\omega)} \right] dz' \quad , \tag{B-6}$$

$$\frac{\partial^2 \Phi}{\partial \mu_i \, \partial \mu_j} = -\operatorname{sgn}\omega \int_0^z \left[\delta_{ij} \left[\frac{1}{\mu_s(z',\underline{\mu};\omega)} + \frac{1}{\mu_s(z',2\underline{k} + \underline{\mu};\omega)} \right] \right. \tag{B-7}$$

$$\left. + \frac{\mu_i \, \mu_j}{\mu_s^3(z',\underline{\mu};\omega)} + \frac{(2k_i + \mu_i)(2k_j + \mu_j)}{\mu_s^3(z',2\underline{k} + \underline{\mu};\omega)} \right] dz' \quad .$$

In these equations, both indices take on the values 1 and 2 and δ_{ij} denotes the Kronecker delta function.

The phase has a stationary point when $\mu_i = -k_i$, $i = 1,2$. The value of the phase at the stationary point provides the phase in the integral in (14). Furthermore,

$$\frac{\exp\{-i\pi(\operatorname{sgn}\omega)/2}{|\omega|} = \frac{1}{i\omega} \tag{B-9}$$

and arrive at (14).

APPENDIX C: ASYMPTOTIC INVERSION FOR ALPHA

In this appendix, we shall derive the result (19) from the integral (17). To do this, we shall first calculate the leading term of the asymptotic expansion of the fourfold integral in the variables $\underline{k}$ and $\underline{x}$. In order to implement the stationary phase formula (B-4), we think of the latter two variables as being k_3 and k_4.

Let us define the phase to be analyzed to be

$$\Phi = 2(\operatorname{sgn}\omega)\int_{\zeta}^{z}\mu_3(z',\underline{k};\omega)\,dz' + 2\underline{k}\cdot(\underline{\xi}-\underline{x}) \quad . \tag{C-1}$$

We take the derivative of this phase function:

$$\frac{\partial\Phi}{\partial k_i} = -2\ (\operatorname{sgn}\omega)\int_{\zeta}^{z}\frac{k_i}{\mu_3}\,dz' + 2(\xi_i - x_i), \quad i = 1,2 \quad ,$$

$$\frac{\partial\Phi}{\partial x_i} = 2k_i, \quad i = 1,2 \quad . \tag{C-2}$$

The conditions that the phase be stationary yield the solution

$$k_i = 0, \quad x_i = \xi_i, \quad i = 1,2 \quad . \tag{C-3}$$

We must now calculate the matrix of second derivatives at the stationary point. This is greatly facilitated by employing (C-3) in the calculation process to disregard contributions which are zero at the stationary point. We find that at the stationary point,

$$\begin{aligned} \Phi_{11} &= \Phi_{22} = -\frac{2}{\omega}\int_{\zeta}^{z} c(z')\, dz' \quad , \\ \Phi_{13} &= \Phi_{24} = \Phi_{31} = \Phi_{42} = 2 \quad , \end{aligned} \tag{C-4}$$

with all other terms being zero. For this matrix, we find that

$$\det \Phi_{ij} = 16, \quad \operatorname{sgn} \Phi_{ij} = 0 \tag{C-5}$$

and

$$\Phi = 2\omega \int_{\zeta}^{z} \frac{dz'}{c(z')} \quad . \tag{C-6}$$

We now use the stationary phase formula (B-4) and find that

$$w(\xi,\zeta) = \frac{c(\zeta)\, c(0)}{\pi} \int_0^\infty dz \int d\omega \, \frac{a(\xi,\zeta)\, \exp\{2i\omega \int_\zeta^z dz'/c(z')\}}{c(z) \int_0^z c(z')\, dz'} \quad . \tag{C-7}$$

The ω integration can now be carried out to yield

$$w(\zeta,\xi) = c(\zeta)\, c(0) \int_0^\infty dz \, \frac{a(\xi,z)\, \delta\left[\int_\zeta^z dz'/c(z')\right]}{c(z) \int_0^z c(z')\, dz'} \quad . \tag{C-8}$$

We now apply to (C8) the rule,

$$\int \delta(f(z))\, g(z)\, dz = \frac{g(\zeta)}{|f'(\zeta)|} \quad , \tag{C-9}$$

with ζ being the only (simple) zero of $f(z)$ in the domain of integration. This yields the result (19).

APPENDIX D: COMPARISON WITH EARLIER RESULT

In this appendix we shall discuss the comparison of (23) with the corresponding result from Cohen and Bleistein [1979a]. In the latter, the formula for α, in the two and one-half dimensional case, is stated in equations (9) and (10). We quote that result with changes in notation to correspond to the notation here: we must interchange the roles of x, ξ and z, ζ. The formula for α then becomes

$$\alpha(\xi,\zeta) = \frac{8ic^2}{\pi} \int dx \int dk_1 \int k_3\, dk_3 \int_0^\infty d\tau \int_0^\tau dt$$

$$\cdot\, \tau(\tau - t)\, U_S(x,0,t)\, \exp\{2i[k_1(\xi - x) - k_3\zeta] + i\omega\tau\} \quad . \tag{D-1}$$

In this equation,

$$\omega = c\, \operatorname{sgn} k_3 \sqrt{k_1^2 + k_3^2} \quad . \tag{D-2}$$

We shall now simplify the time domain integrals. To begin, let us define

$$I = \int_0^\infty d\tau \int_0^\tau dt\tau(\tau - t)\, U_S(x,0,t)\, \exp\{i\omega\tau\} \quad . \tag{D-3}$$

In this integral, we wish to interchange the order of integration. In doing so, we take the point of view that ω has a positive imaginary part. Indeed, there is justification for this. The original problem was "causal;" that is, the experiments were carried out starting from some finite time. Thus, the Fourier transform to frequency domain is originally defined and analytic in some upper half ω-plane. Before analytically continuing the transform down to the real axis, the interchange is justified. After carrying out the interchange, we obtained

$$I = \int_0^\infty dt\, U_S(x,0,t) \int_t^\infty \tau\, d\tau(\tau - t)\, \exp\{i\omega\tau\} \quad . \tag{D-4}$$

We now calculate the τ integral by integrating by parts and keeping the leading order term in ω for large $|\omega|$. The result is

$$I = \frac{1}{\omega^2} \int_0^\infty dt\; t\, U_S(x,0,t)\, \exp\{i\omega t\} \quad , \tag{D-5}$$

which we can also write as

$$I = \frac{1}{i\omega^2} \frac{\partial}{\partial \omega} \int_0^\infty dt\ U_S(x,0,t)\ \exp\{i\omega t\} \quad . \tag{D-6}$$

We substitute this result into (D-1) and also introduce the change of variable of integration from k_z to ω via the equation

$$k_z = \text{sgn}\ \omega \sqrt{\frac{\omega^2}{c^2} - k_x^2} \quad , \tag{D-7}$$

and obtain

$$\alpha(\xi,\zeta) = \frac{8c}{\pi} \int dx \int dk_x \frac{d\omega}{\omega} \exp\{2i[k_x(\xi - x) - k_z\zeta]\}$$
$$\cdot \frac{\partial}{\partial \omega} \int_0^\infty U_S(x,0,t)\ \exp\{i\omega t\}\, dt \quad . \tag{D-8}$$

The theory developed in Cohen and Bleistein [1979a] indicates that we obtain the reflectivity function by multiplying the integrand by $2i\omega/c$, which yields the following result:

$$\beta(\xi,\zeta) = \frac{\partial \alpha(\xi,\zeta)}{\partial n} = \frac{16i}{\pi} \int dx \int dk_x \int d\omega\ \exp\{2i[k_x(\xi - x) - k_z\zeta]\}$$
$$\cdot \frac{\partial}{\partial \omega} \int U_S(x,0,t)\ \exp\{i\omega t\}\, dt \quad . \tag{D-9}$$

An integration by parts in ω now yields the result

$$\beta(\xi,\zeta) = -\frac{32\zeta}{\pi c^3}\int dx \int dk_1 \int \frac{\omega\, d\omega}{k_3} \exp[2i[k_1(\xi - x) - k_3\zeta]] \tag{D-10}$$

$$\cdot \int_0^\infty dt\; U_S(x,0,t)\; \exp[i\omega t]\, dt \quad .$$

When (23) is specialized to the case of constant c, the result is exactly the same as (D-10) when one makes the identification

$$\mu_3 \; \text{sgn}\; \omega = k_3 \; . \tag{D-11}$$

APPENDIX E: ASYMPTOTIC EXPANSION OF THE SOLUTION FORMULA

We shall describe here the asymptotic expansion by the method of stationary phase of the integral with respect to k in (23). We begin by rewriting that inegral as

$$\beta(\xi,\zeta) = -\frac{32\int_0^\zeta c(z)dz}{\pi c^2(\zeta)c(0)} \int |\omega| d\omega \int dx \int dt\ U_S(x,0,t) \tag{E-1}$$

$$\cdot \int \frac{dk\ \exp\{2i\bar{\xi} + i\omega t\}}{\mu_s(z,k;\omega)} .$$

In this equation,

$$\bar{\xi} = k(\xi - x) - \operatorname{sgn}\omega \int_0^\zeta \mu_s(z,k;\omega)\, dz. \tag{E-2}$$

To calculate this integral by the method of stationary phase, we need the first and second derivatives of the phase function. They are given by

$$\frac{\partial\bar{\xi}}{\partial k} = \xi - x + k \operatorname{sgn}\omega \int_0^\zeta \frac{dz}{\mu_s(z,k;\omega)} \tag{E-3}$$

and

$$\frac{\partial^2 \Phi}{\partial k^2} = \int_0^\zeta \frac{dz}{c^2(z)\mu_3^3(z,k;\omega)} \quad . \tag{E-4}$$

The condition that the phase be stationary, that is, that $\partial\Phi/\partial k = 0$, is

$$x - \xi = k \operatorname{sgn}\omega \int_0^\zeta \frac{dz}{\mu_3(z,k;\omega)} \quad . \tag{E-5}$$

We set

$$k = \frac{\omega}{c_0} p \operatorname{sgn}(x - \xi) \tag{E-6}$$

and then (E-5) is just the ray equation, which is the first equation in (25). Furthermore, at the stationary point,

$$\mu_3(z,k,\omega) = \frac{|\omega|}{c(0)} \sqrt{n^2(z) - p^2} \quad , \quad \Phi = \omega\tau(p,\zeta) \quad ,$$
$$\frac{d^2\Phi}{dk^2} = c(0)\,\omega^2\, S(\zeta,p) \operatorname{sgn}\omega \quad . \tag{E-7}$$

Substitution of these values and application of the stationary phase formula to (E-1) yields the result, (24), (25).

APPENDIX F: SAMPLING RATE OF OUTPUT IN DEPTH

We shall discuss here the question of the sampling rate in depth of the output of a seismic inversion algorithm. These considerations are not peculiar to inversion; they apply to any similar imaging technique.

Let us consider the final step of the integral process to image a reflector. For simplicity we deal with the case of a horizontal reflector in one spatial dimension. Then, the last integral to be performed is of the form

$$I(z) = \int_B \exp\{4\pi i f z/c\}\, df \quad . \tag{F-1}$$

In this equation, the band B over which the integral is to be calculated is a symmetric pair of intervals, $(-f_+, -f_-)$, (f_-, f_+). Calculating this integral explicitly and using a trigonometric identity for the difference of sines of two angles yields the result

$$I(z) = \frac{c \cos[2\pi(f_+ + f_-)z/c] \sin[2\pi(f_+ - f_-)z/c]}{\pi z} \quad . \tag{F-2}$$

The zeroes of this function nearest to the origin occur when the cosine factor in this equation is zero or when the argument of the cosine factor is $\pi/2$. The distance between these two zeroes is determined by setting the argument of the cosine equal to π.

On empirical grounds, we require that the sampling rate in depth be such that there are four sample points in this interval. Therefore, if Δz is the sample interval,

$$\frac{2\pi(f_+ + f_-)\, 4\,\Delta z}{c} = \pi \quad ; \tag{F-3}$$

or,

$$\Delta z = \frac{c}{8(f_+ + f_-)} \tag{F-4}$$

Let us define the maximum depth to be Z and the maximum time corresponding to that depth, to be T. Then, neglecting the practical aspects of processing to the maximum depth, we set

$$N_z = \frac{z}{\Delta z} = 4\Delta t(f_+ + f_-)\, N_t \quad . \tag{F-5}$$

For a sample rate of 4 mils and a useful frequency range of 5-30 Hz, we obtain from (F6) the estimate, $N_z/N_t = .56$.

FIGURE CAPTIONS

Figure 1. The bandlimited singular function of a surface.

Figure 2(a). Synthetic time section: dipping planar reflector in a medium where the velocity increases linearly with depth. Dip angle is 60 degrees; velocity is (5000 + 4z) ft/sec.

Figure 2(b). Depth section reconstructed via the Born procedure. The reflector has been properly located.

Figure 2(c). Depth section reconstructed via Kirchhoff migration using rms velocities. Because of errors in computing traveltimes for diffraction curves, the result is a severe overmigration.

Figure 3(a). Salt dome model.

Figure 3(b). Synthetic time section.

Figure 3(c). Reconstructed depth section. All dips up to 90 degrees have been properly migrated.

Figure 3(d) Output of Whitmore's reverse-time finite difference migration. (With the permission of the author.)

Figure 4(a). Salt dome model with ray paths from one reflecting horizon.

Figure 4(b). Synthetic time section.

Figure 4(c). Reconstructed depth section.

Figure 4(d). Reconstructed depth section; the anti-aliasing constraint (28) has been modified.

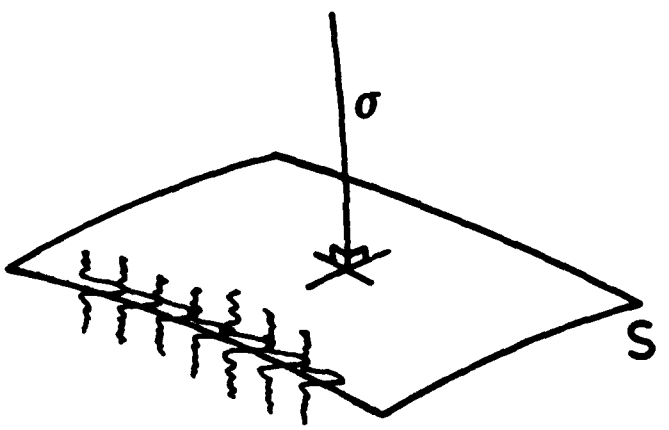

$$\gamma(\mathbf{x}) = \delta(\sigma)$$

FIGURE 1

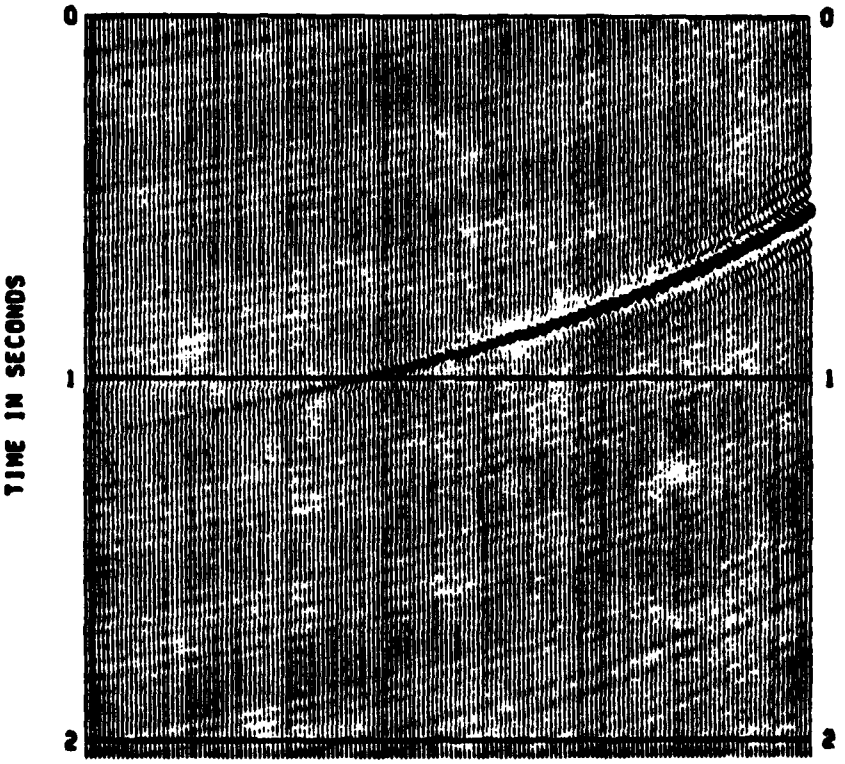

FIGURE 2A

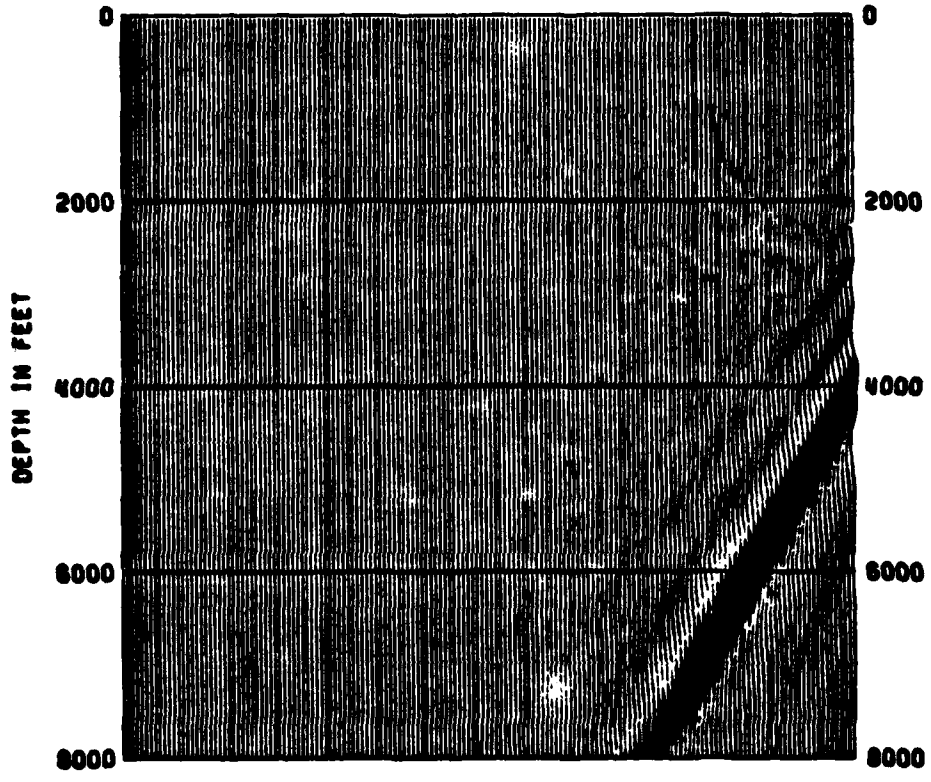

FIGURE 2B

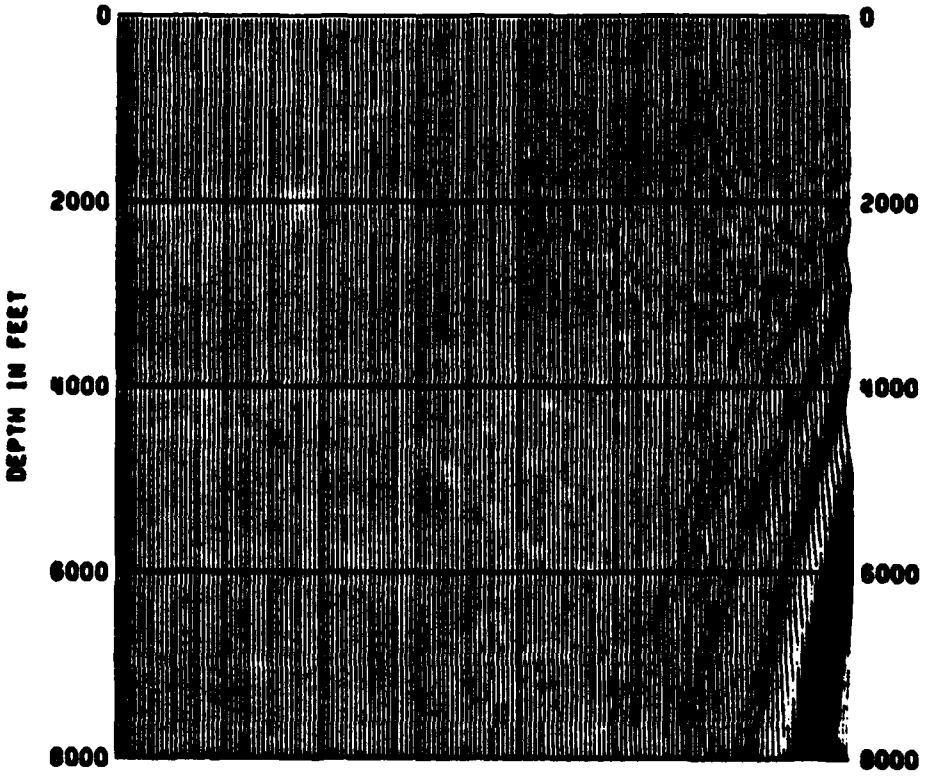

FIGURE 2C

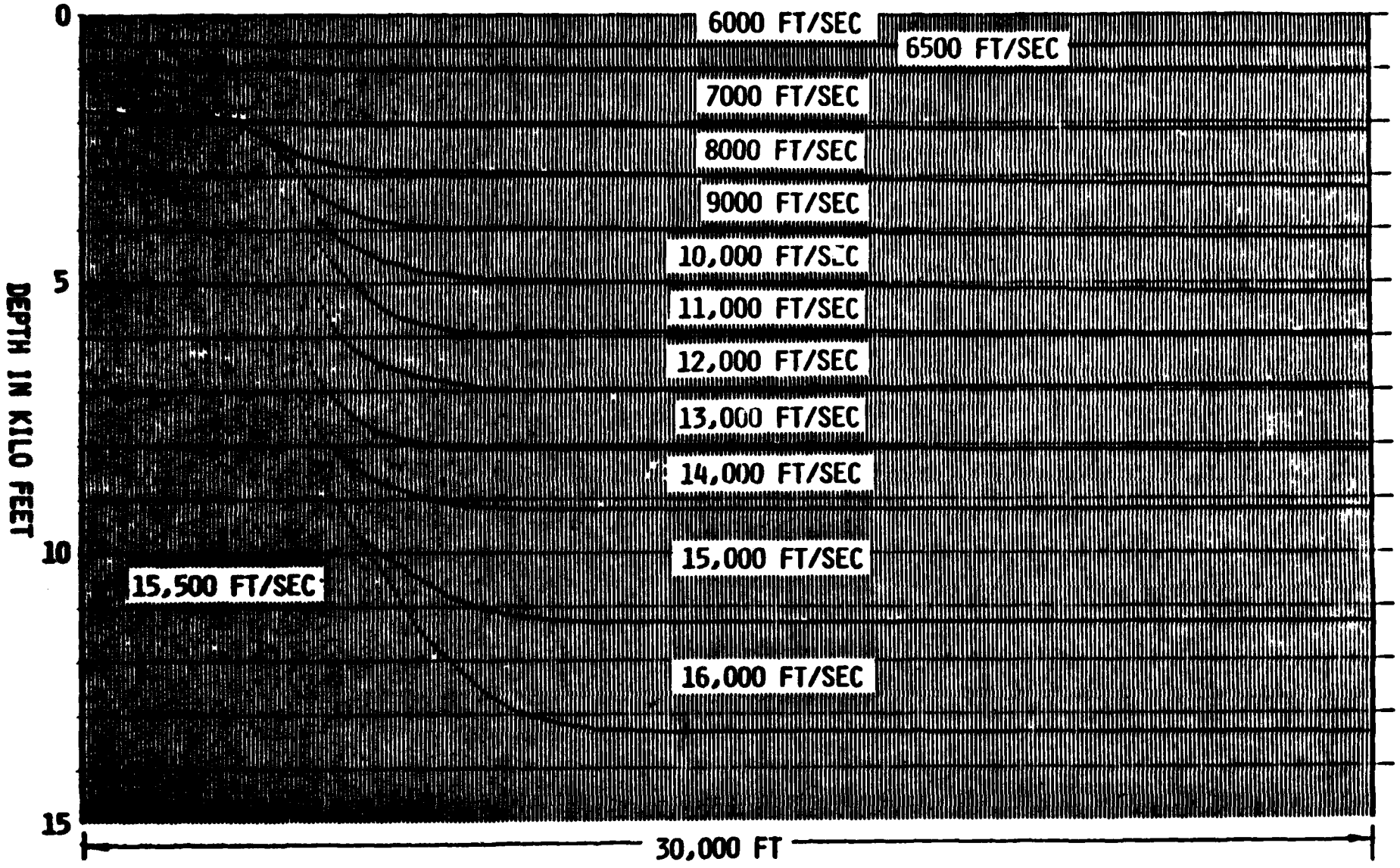
0
5
10
15
DEPTH IN KILO FEET
6000 FT/SEC
6500 FT/SEC
7000 FT/SEC
8000 FT/SEC
9000 FT/SEC
10,000 FT/SEC
11,000 FT/SEC
12,000 FT/SEC
13,000 FT/SEC
14,000 FT/SEC
15,000 FT/SEC
15,500 FT/SEC
16,000 FT/SEC
30,000 FT

FIGURE 3A

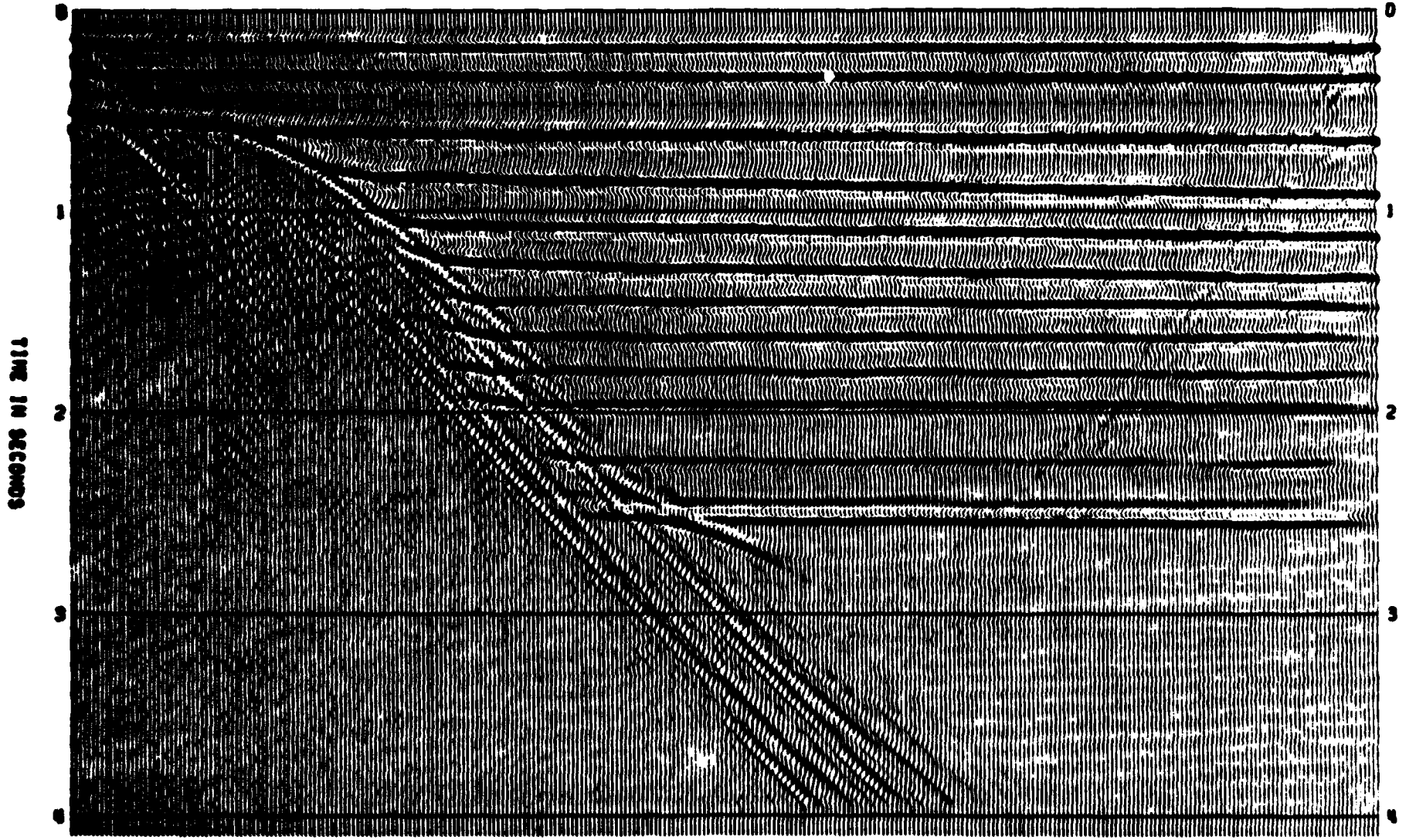

FIGURE 3B

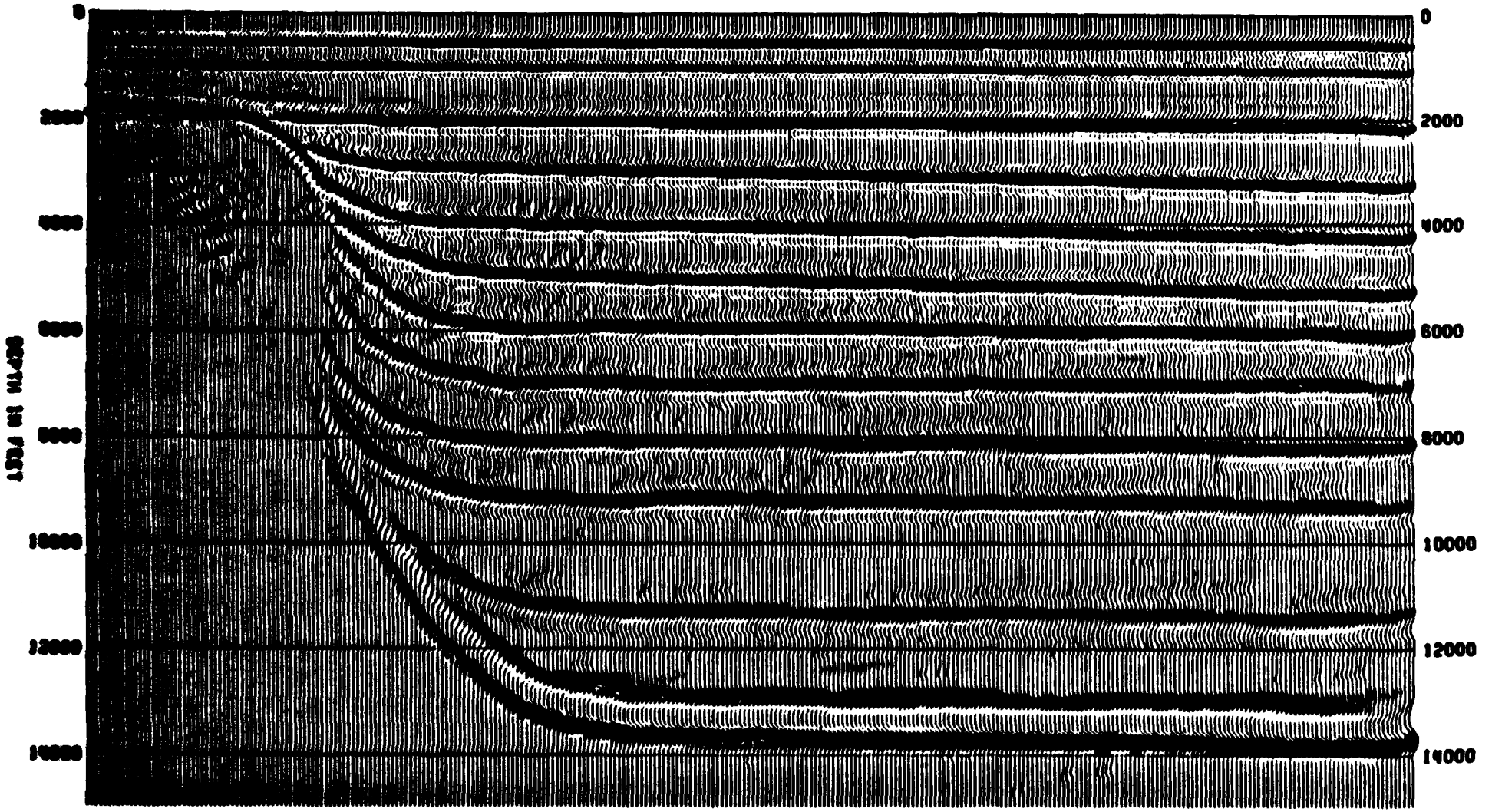

FIGURE 3C

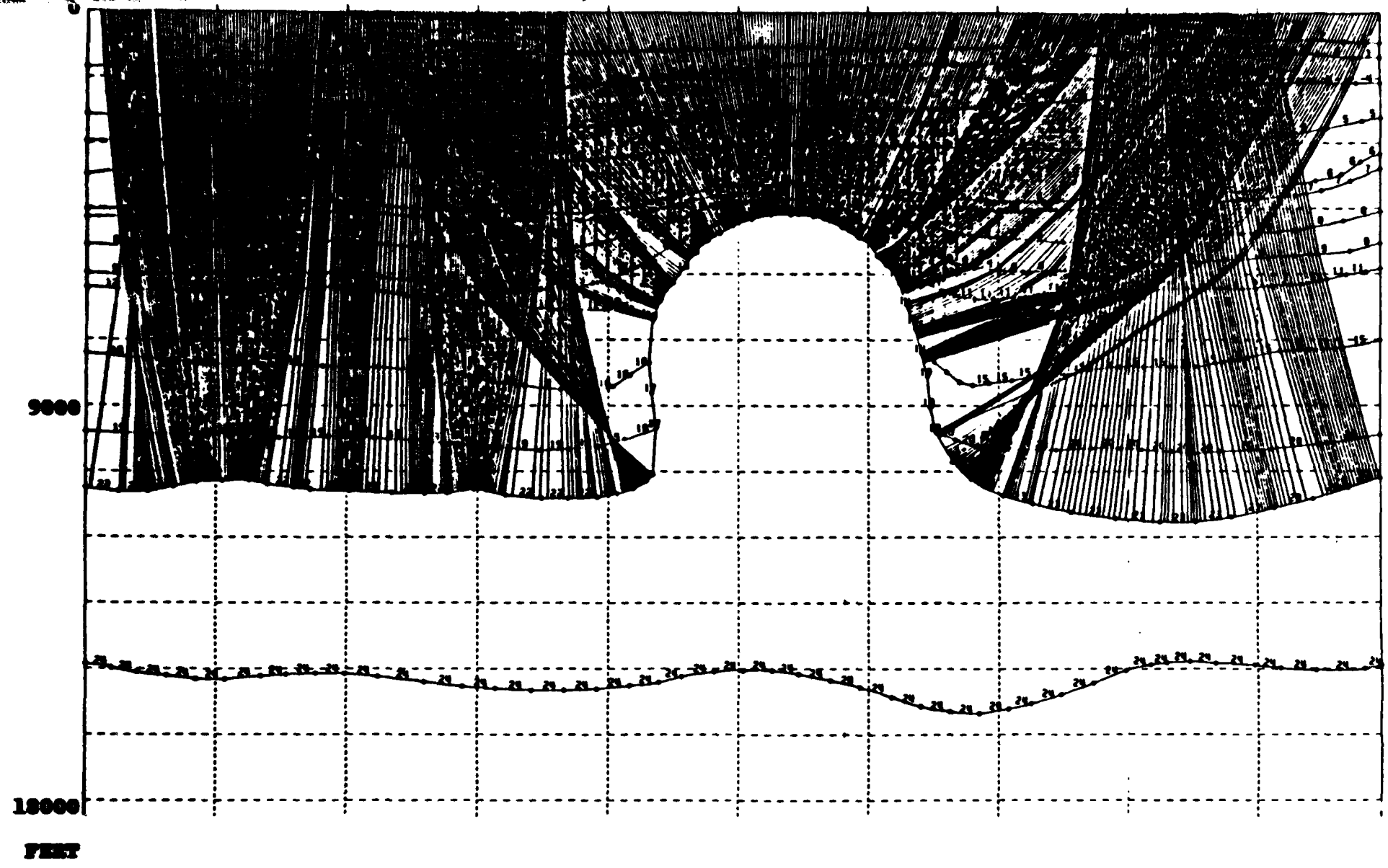

FIGURE 4A

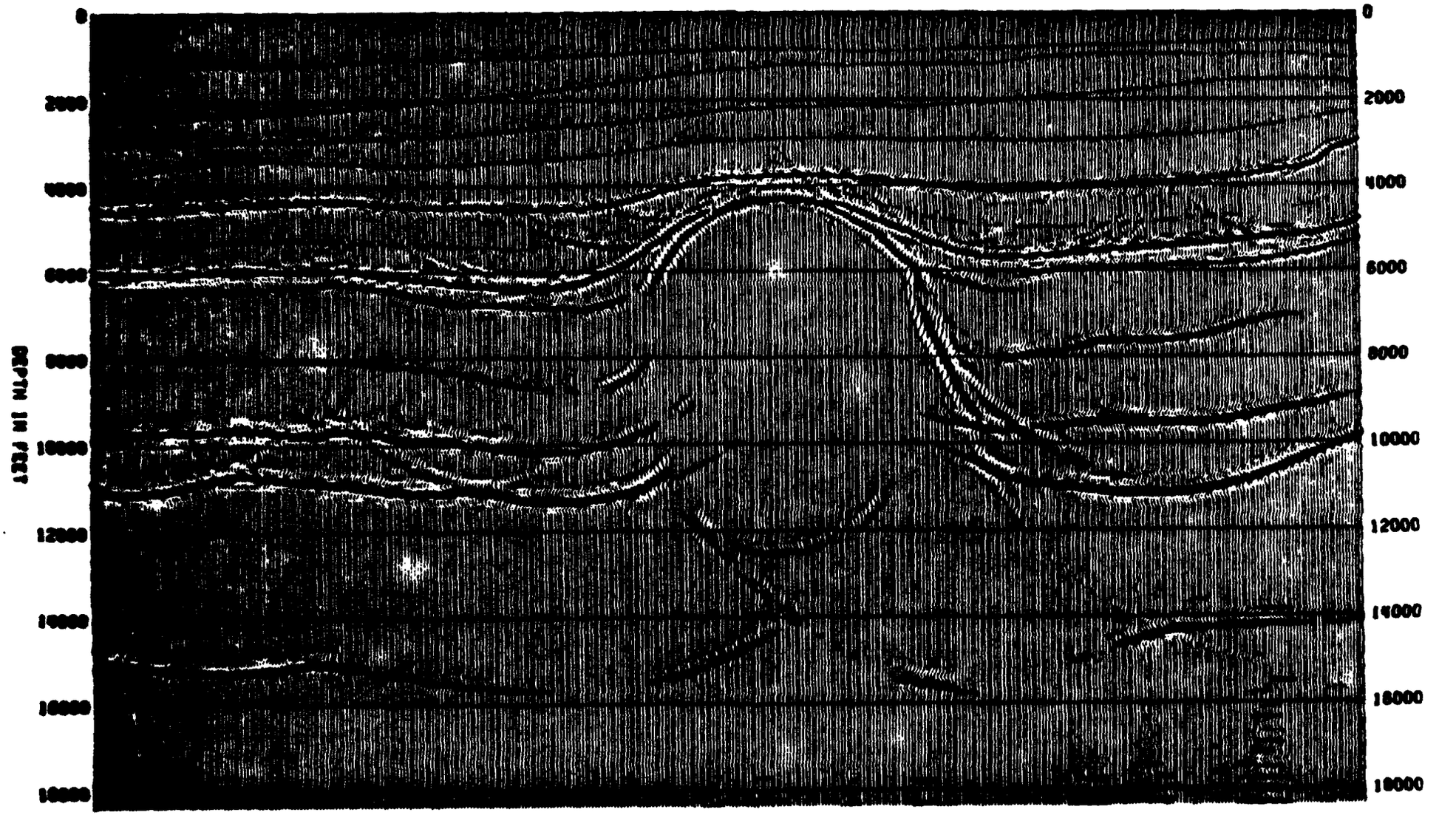
0
2000
4000
6000
8000
10000
12000
14000
16000
18000
DEPTH IN FEET

FIGURE 4C

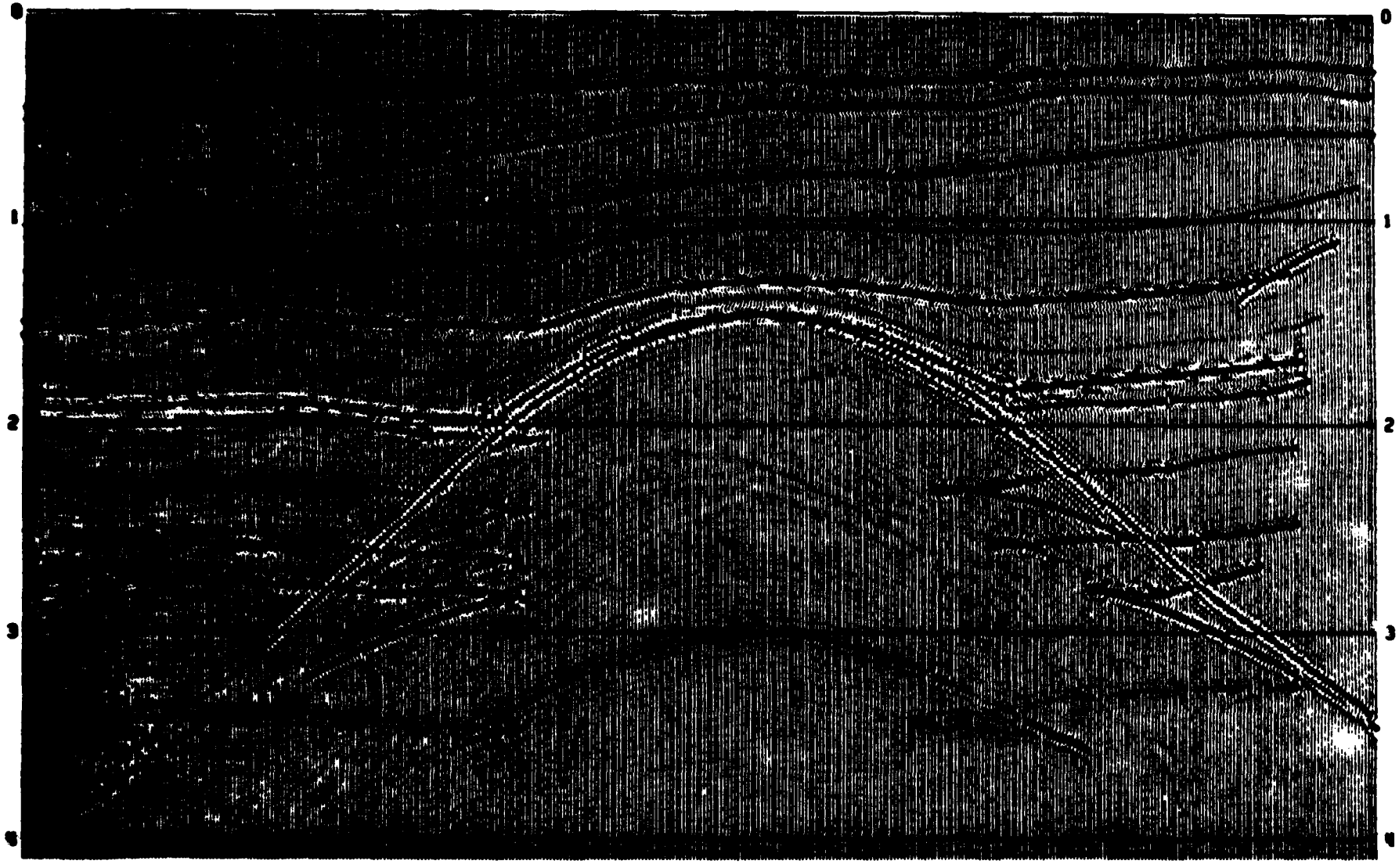

FIGURE 4B

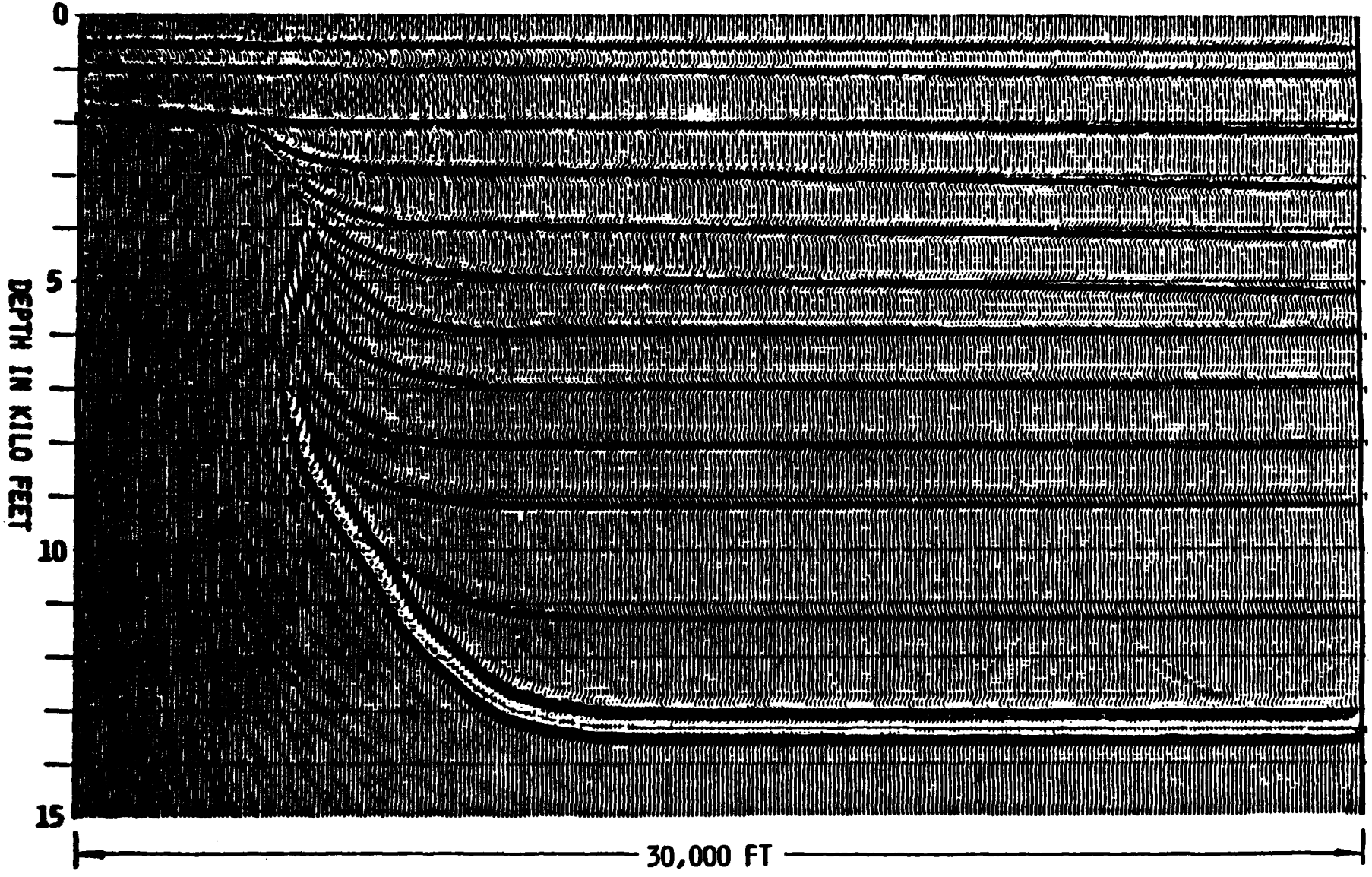

FIGURE 3D

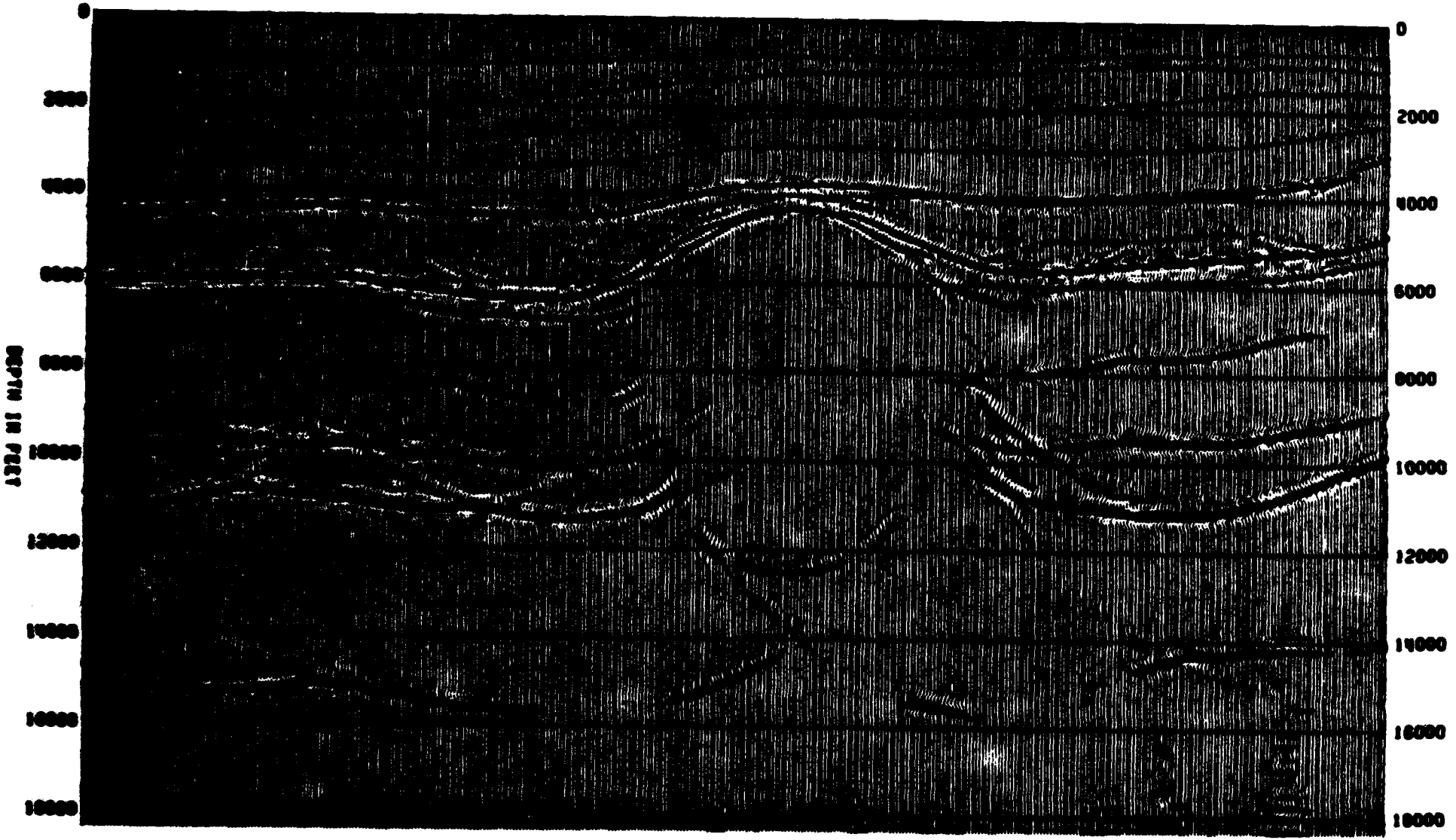

FIGURE 4D

unclassified

415077

SECURITY CLASSIFICATION OF THIS PAGE (When Data Entered)

REPORT DOCUMENTATION PAGE		READ INSTRUCTIONS BEFORE COMPLETING FORM
1. REPORT NUMBER CWP-007	2. GOVT ACCESSION NO. ADA146469	3. RECIPIENT'S CATALOG NUMBER
4. TITLE (and Subtitle) An Extension of the Born Inversion Method to a Depth Dependent Reference Profile		5. TYPE OF REPORT & PERIOD COVERED Technical
		6. PERFORMING ORG. REPORT NUMBER
7. AUTHOR(s) Norman Bleistein and Samuel H. Gray		8. CONTRACT OR GRANT NUMBER(s) N00014-84-K-0049
9. PERFORMING ORGANIZATION NAME AND ADDRESS Center for Wave Phenomena Department of Mathematics Colorado School of Mines, Golden, CO 80401		10. PROGRAM ELEMENT, PROJECT, TASK AREA & WORK UNIT NUMBERS NR SRO-157/83SEP02 (410
11. CONTROLLING OFFICE NAME AND ADDRESS Office of Naval Research Arlington, VA 22217		12. REPORT DATE August 1, 1984
		13. NUMBER OF PAGES 67
14. MONITORING AGENCY NAME & ADDRESS(if different from Controlling Office)		15. SECURITY CLASS. (of this report)
		15a. DECLASSIFICATION/DOWNGRADING SCHEDULE

16. DISTRIBUTION STATEMENT (of this Report)

This document has been approved for public release and sale; its distribution is unlimited.

17. DISTRIBUTION STATEMENT (of the abstract entered in Block 20, if different from Report)

18. SUPPLEMENTARY NOTES

19. KEY WORDS (Continue on reverse side if necessary and identify by block number)

Born inversion	imaging
velocity inversion	depth dependent background
singular function	stationary phase
reflectivity function	WKB

20. ABSTRACT (Continue on reverse side if necessary and identify by block number)

See other side.

DD FORM 1 JAN 73 1473 EDITION OF 1 NOV 65 IS OBSOLETE S/N 0102-014-6601 | unclassified SECURITY CLASSIFICATION OF THIS PAGE (When Data Entered)

ABSTRACT

The purpose of this paper is to describe an extension of the multidimensional Born inversion technique [Cohen and Bleistein, 1979a] for acoustic waves. In that earlier work, a perturbation in reference soundspeed was determined by assuming that the reference or background speed was constant. In this extension, we allow the reference speed to be a function of the depth variable, z, but still require that it be independent of the transverse variables. The output of this method is a high frequency bandlimited reflectivity function of the subsurface. The reflectivity function is an array of bandlimited singular functions scaled by the normal reflection strength. Each singular function is a Dirac delta function of a scalar argument which measures distance normal to a reflecting interface. Thus, the reflectivity function is an indicator map of subsurface reflectors which is equivalent to the map produced by migration. In addition to the assumption of small perturbation, the method requries the assumption that the reflection data reside in the high frequency regime, in a well-defined sense.

The method is based on the derivation of an integral equation for the perturbation in soundspeed from a known reference speed. When the reference speed is constant, the integral equation admits an analytic solution as a multifold integral of the reflection data. Further high frequency asymptotic analysis simplifies this integral considerably and leads to an extremely efficient numerical algorithm for computing the relfectivity function. In a paper by Bleistein, Cohen and Hagin [1984], the development of a computer code to implement this constant reference speed solution is described.

For a depth dependent reference speed, c(z), we can no longer invert the integral equation exactly. However, we can write down an asymptotic high frequency approximation for the kernel of the integral equation and an asymptotic solution for the perturbation. The computer implementation of this result is designed along the same lines as the code for the constant background case. In tests of processing time, we find that, at worst, the total processing time for this algorithm with depth dependent background soundspeed is about the same as for a comparably programmed k-f algorithm with constant background. By worst we mean that we choose the aspect ratio — the number of traces divided by the number of points per trace — to be optimal for the k-f algorithm. We present examples which demonstrate the method implemented as a migration technique and compare with the application of alternative migration algorithms. The examples we chose were ones in which the objective is to image the flanks of a salt dome.